1958

Behavior of welded corner connections, Welding Journal, 37 (5), p. 216-s, (1958), Reprint No. 122 (58-2)

J. W. Fisher

G. C. Driscoll Jr.

F. W. Schutz Jr.

Welded Continuous Frames and Their Components
Progress Report No. 23

BEHAVIOR OF WELDED CORNER CONNECTIONS

by

John W. Fisher
George C. Driscoll, Jr.
F. W. Schutz, Jr.

This work has been carried out as part of an investigation sponsored jointly by the following:

American Institute of Steel Construction
American Iron and Steel Institute
U. S. Navy Department (Contracts 39303 and 610(03))
Office of Naval Research
Bureau of Ships
Bureau of Yards and Docks
Welding Research Council

August, 1957

Fritz Engineering Laboratory
Department of Civil Engineering
Lehigh University
Bethlehem, Pennsylvania

Fritz Laboratory Report No. 205C.21

C O N T E N T S

A B S T R A C T

The results of a series of tests on straight corner connections for welded rigid portal frames are reported in this paper. These connections were proportioned using the concepts of plastic analysis. The purpose of this study was to determine the effect of member size on connection behavior. It was desirable to know if connections fabricated of larger size rolled sections would meet the "requirements" for connections which had been established in earlier studies using small specimens.

The knees were tested in a universal testing machine in a manner that simulated forces and moments tending to close the connection. Measurements were made to determine the rotation in the vicinity of the plastic hinge, the relative deflection between ends of the legs, the magnitude of the lateral support forces, and commencement of local web and flange buckling.

Theoretical expressions used in the calculation of the forces and deformations are described. From these expressions it is possible to correlate theory with the test results.

The factors leading to the design of the stiffening which includes the end plate, diagonal stiffener, and vertical stiffener are discussed. The welds were proportioned to carry plastic moments and forces. The sequences used for welding the test specimens in order that induced stresses and distortion could be minimized are outlined.

A comparison between welds proportioned in this manner and those proportional by present day weld procedures is given. This showed the

only weld which is larger by "plastic" design is the column web fillet weld to the beam flange.

The results of test carried out on connections using 14WF30, 24WF100, 30WF108 and 36WF230 rolled sections are presented. These welded connections were of the same general proportions as may be found in present day construction. The results of earlier experimental work on the same type connection fabricated from 8B13 sections is included for comparison.

The tests showed that changing the size of member has no adverse effect on the performance of the type connection tested. It was found that connections of large size members are able to absorb a sufficient amount of rotation after reaching maximum moment provided adequate lateral support is furnished.

It can be concluded that the results of earlier theoretical and experimental work on small members can be applied to the larger rolled sections.

Equations and sample calculations for use in design are presented in an Appendix.

1. INTRODUCTION

1. OBJECT AND SCOPE OF INVESTIGATION

A series of tests were carried out at Lehigh University as the second phase of a program on corner connections which is part of the broad investigation titled "Welded Continuous Frames and Their Components".

The earlier phase covered the testing of a number of corner connections of different designs, all connecting 8 B 13 members. The purpose of the tests was to determine whether the different types of knees being studied would show performance satisfactory for their use in structures designed by either plastic or elastic analysis. Among the problems studied were the strength, stiffness, rotation capacity, and economy of fabrication.(1)

In the second phase, the effect of size of member on connection behavior is discussed. The test specimens were "type 8B" as classified in the original study. As shown in Fig 1, they were straight knees with diagonal stiffeners and half-depth vertical stiffeners. The rolled sections originally intended for study were the 14WF30, 24WF100, and 36WF230. These rolled sections were chosen on the basis of their geometric similarity to the 8 B 13 used in the earlier tests. It was decided also to include the results of a 30WF108 connection tested later but which did not have geometric similarity to the other connections tested. The type 8B connection was selected because it showed good behavior in the elastic and plastic range in the earlier tests and was economical to fabricate.

Measurements made during the tests were used to determine whether the knee would meet the requirements for knees in structures. These requirements had been established in an earlier study.[1] They are:

(a) The knee must be capable of resisting at the corner the full plastic moment, M_p, of the rolled sections joined.

(b) The stiffness should be at least as great as that of an equivalent length of the rolled sections joined.

(c) The knee should have sufficient rotation capacity; that is, it should be capable of absorbing further rotations at near - maximum moments after reaching the plastic hinge condition.

(d) The knee should be economical to fabricate.

2. DESCRIPTION OF KNEES AND TESTING APPARATUS

2. TEST SPECIMENS

Each specimen consisted of two identical members joined at right angles. As is shown in Fig 1, the end of the web of the column was joined to the lower flange of the beam. An end plate equal in cross section to the nominal section of the flange was used to prolong the outer flange of the column to meet the top flange of the beam. Two types of end plates were used, one incorporating an overlap, and the other butting the column flange. Diagonal stiffeners of thickness equal to the nominal flange thickness extended from the intersection of outer flanges to the intersection of inner flanges. Sniped half-depth vertical stiffeners were added as a prolongation of the inner flange of the column. The lengths of both legs were equal and were about four times the section depth. This provided a reasonable ratio of shear to moment and axial force to moment. It was necessary to make the legs of the 14WF30 about six times the section depth to provide testing clearances in the testing machine.

In Fig 2 the cross sections of the four rolled shapes are drawn to scale along with the 8 B 13 cross section used in the earlier tests. A-7 structural steel was the material from which the sections were rolled. The properties of the various pieces of rolled shape and plate material used in fabricating the specimens were determined from coupons cut from these sections. The tensile specimens were tested in a hydraulic universal testing machine at a slow laboratory rate. Load and elongation over an 8-inch gage length were measured and plotted by means of a low-magnification

automatic stress-strain recorder. The rate of application of load was about 30 micro-inches per inch per second in the plastic range, a rate much lower than the usual standard mill test rate. This reduced rate of loading was used because the results were to be applied to predict values for static tests where equilibrium of load and deformation would be obtained at each load increment before readings would be taken. Fig 3 shows an idealized stress-strain curve obtained from tension coupons and defines the various terms used in Table 1. The results of the tests carried out on these coupons may be seen in Table 1. Compression coupon tests were also conducted. For a more comprehensive outline of testing procedure and how the various quantities are measured, see Ref 2. The results of the mill tests are also shown in Table 1.

For theoretical calculations, average coupon values were used. These values were obtained by taking a weighted average of the coupon tests results in proportion to the flange and web areas.

The cross-section dimensions of each specimen were measured and recorded for comparison with handbook[3] values, and for use in making theoretical calculations. A summary and comparison of these values is shown in Table 2.

The chemistry of the steel was such that even with the thick flanges of the larger sections, it was possible to weld without preheating or using special electrodes.[4]

3. LOADING SYSTEM

In the connection tests, the knees were set up in an 800,000 lb. universal screw-type machine in the position shown in Fig 4. The connections were tested by the scheme shown in Fig 5. Considering the

legs of the knee as the legs of a 45° - 45° - 90^otriangle, concentrated loads were applied along the hypotenuse of the triangle. The effect of this loading condition on the knee itself was to cause bending moments which were maximum at the corner, plus equal shear and thrust forces in the order of magnitude of about 10% of the theoretical stub-column yield load.

End bearing at the points of load application was supplied through steel pins 12 inches long welded perpendicular to the plane of the web. These pins were able to rotate in the plane of the connection on the flat bearing surfaces attached to the testing machine. Thus, a condition of zero moment was assumed at the points of load application. The necessary horizontal reactions to prevent overturning of the knee assembly due to its own weight were supplied by friction once a small load was applied. As a safety precaution, restraining devices were positioned so as to support the structure should slip occur.

The end bearing pins and web of the specimen were stiffened by doubler plates and stiffeners which also were designed to carry part of the end reaction to the flanges.

4. LATERAL SUPPORT

Lateral support for each knee was provided by a system of 4 tie rods attached to the inner and outer corners of the knees at the tips of the flanges. The points of lateral support are shown in Fig 5. The tie rods were arranged so as to restrain the knees from any lateral deflection without interferring with vertical movement between the end pins. The reactions of the lateral supports were carried by a framework

of 14WF30 beams bolted to the fixed columns of the testing machine. (see Fig 4) The bracing frame formed a horizontal plane passing through the corners of the knee. It was designed to take almost all the lateral forces in the system so that the testing machine columns carried only the weight of the framework.

Each tie rod had a turnbuckle to permit adjustment of the forces. An SR-4 electrical strain gage bridge was mounted on each tie rod so that the force could be determined at any time.

Two methods were used to allow freedom of vertical movement of the knee. In the tests of the 14WF30 and the 24WF100, the tie rods were fitted with flex bars at each end. (Fig 6) In the test of the 36WF230, and 30WF108 the tie rods were fitted with pins and clevices at each end. (Fig 25)

5. ROTATION MEASUREMENTS

Measurements of the rotation across the knees and along parts of each leg adjacent to the knee were made by rotation indicators similar to those shown in Fig 6. The development and use of this type of rotation indicator has been described in ref 5.

6. DEFLECTION MEASUREMENTS

The relative deflection of the ends of the legs was measured by a dial gage attached to a rod which spanned the hypotenuse of the triangle formed by the legs of the knee. (Fig 5)

Changes in the average length of the moment arm were measured by means of a "mirror gage". This consisted of a plumb bob attached by a

fine wire to the outside corner of the knee and a 1/100 inch scale equipped with a mirror. The movement of the wire was measured against the scale.

Lateral motion of the knee was measured either by dial gages referenced to the fixed columns of the testing machine or by means of mirror gages.

7. FLANGE AND WEB BUCKLING MEASUREMENTS

In order to detect local flange and web buckling of the rolled sections before buckling was visible to the eye, deflection measurements were taken at a number of uniformly spaced stations along each member.

Flange buckling was detected by measuring the relative displacement between the fillet of the tension flange and a point about 1/2 inch from the edge of the compression flange. Readings were taken with a dial gage equipped with extended points of proper length to span the diagonal distance. The points were held firmly in punch marks at each gage station by hand, and the gage was moved from station to station for each set of readings. The gage is shown schematically in Fig 22.

The displacements of points on the center line of the web with respect to a line across the tips of the flanges were measured with a web buckling detector. The detector was a dial gage attached at right angles to a steel bar long enough to span the flanges. (see Fig 23) The dial gage was equipped with an extender point. As with the flange buckling detector, the gage was hand held while readings were being taken.

With both the flange and the web buckling detectors, a set of reference stations was maintained on an unloaded section of beam as a check against accidental changes in the setting of the dial.

These readings were not made on the 30WF108.

8. TEST PROCEDURE

In the conducting of each test, four phases of the test required slightly different procedures. Those phases were:

(a) Initial adjustment of test apparatus and instruments and taking of zero readings.

(b) Elastic range loading with load and deformation readings controlled by a deflection criterion.

(c) Plastic range loading with load and deformation readings controlled by a deflection criterion.

(d) Plastic range loading after maximum load with a minimum of deformation readings.

(a) Initial Adjustment

Prior to actual testing, the lateral support tie bars were positioned so that after an inch of downward deflection of the knee they would be horizontal. This would cause a shortening of the tie bars. Consequently, each tie bar was tightened to an equal initial tensile load so that there would be a net tensile load after some deflection.

Once the adjustment of the tie bars was satisfactorily achieved, initial readings were taken of the load, all deflection gages, all SR-4 gages, and all rotation indicators.

(b) Elastic Range Loading

Load increments of approximately 5% of the calculated yield load were applied during the portion of the test in which the deflection of

the ends of the legs and the load increased proportionally. After each load increment had been applied, all deflection, rotation and SR-4 readings were taken. At the completion of each set of readings, the specimen was inspected for any signs of yielding. A coat of whitewash had been applied to the specimen so that flaking of mill scale might be detected more easily. When flaking of mill scale did show some evidence of yielding, a note to this effect was recorded and a sketch showing its location was made. Readings of the flange and web buckling detectors were taken at only a few of the load increments during this part of the test since they did not show significant changes. A running plot of load versus deflection and rotation was made during the test.

During this phase of the test, a reading of load and deflection taken after the initial set of readings would show negligible difference from those recorded at the start of the set of readings 10 or 15 minutes earlier.

This procedure was continued until the specimen had yielded enough for the load to become "unstable" as plastic flow occurred and required much greater amounts of straining to increase the load. Then the procedure was changed to the plastic range procedure using a deflection criterion.

(c) Plastic Range Loading (Up to Maximum Load)

Once the rate of change of deformation with respect to load increased significantly, it became obvious that the criterion for taking readings should be changed.

Since a screw-type testing machine was being used, a given amount of deflection could be applied. Then after sufficient time had elapsed for plastic flow to take place, the load would settle to a fairly stable value. Deflection increments were arbitrarily chosen such that the distance

between plotted points on the load-deflection plot was about the same as that during the elastic portion of the test.

Following the application of an increment of deformation, readings of load, deflection, and time would be taken until the load changed less than 500 pounds and the deflection less than 0.001 inch after 5 minutes. Then all deflection, rotation, buckling detector, and SR-4 gage readings were taken. The progress of any whitewash patterns was also recorded.

In this portion of the test, it was frequently necessary to reset dial indicators which neared the end of their travel. It was also necessary to readjust the lateral support tie rods when excessive deflection of the knee tended to increase the length of the tie bars. This produced forces approaching the capacity of the bars. The rods were loosened and the outer ends were slid along the lateral support beam, after which the rods were tightened to a moderate load.

The "deform - wait - and read" procedure was continued until the maximum load had been reached and the load started to drop off with continuing deformation. By this time most of the gages had reached their limits and either were removed or the taking of readings was discontinued.

(d) Plastic Range Loading (Past Maximum Load)

After the maximum load was reached, the main points of interest were to find how much rotation the knee could withstand, whether local or lateral buckling would cause a catastrophic collapse, and whether any welds would fracture.

The deflection increments were increased to 1/2 inch or 1 inch. Only readings of load, deflection, time, and lateral support force were taken. When the load fell below the predicted yield load, the test was terminated.

3. THEORETICAL ANALYSIS

To meet the requirements for performance of knees in structures, the connection must be able to transmit the forces and displacements of the members joined. Excessive shear deformation within the knee must be prevented. The following chapter describes the theoretical expressions used in the calculation of the forces and displacements. Expressions are also presented for the reinforcement required within the knee to prevent excessive deformation.

9. YIELD MOMENT AND PLASTIC MOMENT OF CROSS SECTION

For use as parameters in plotting non-dimensionalized curves and for proportioning the knees, values of the yield moment, M_y, and the plastic moment, M_p, are calculated for the rolled section.

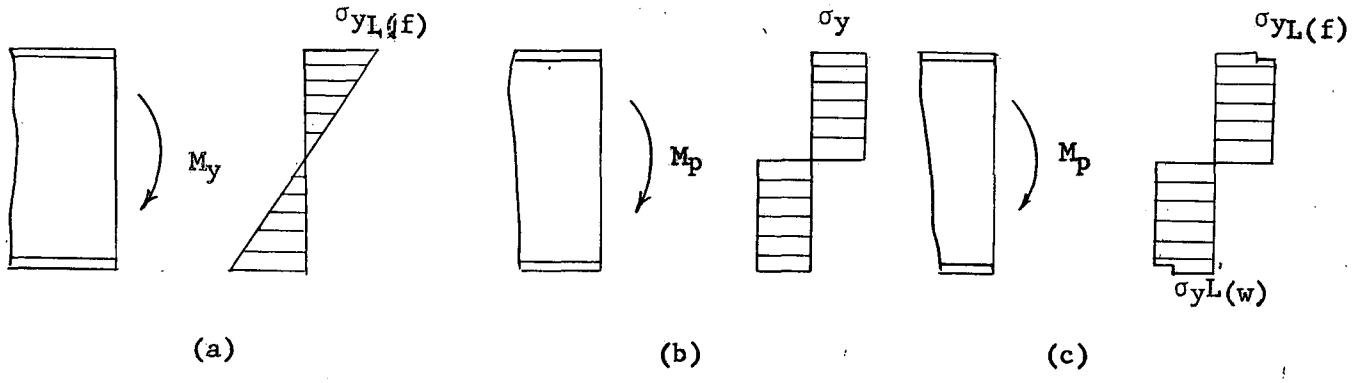

Fig. 7

The yield moment due to the stress distribution in Fig 7a is

$$M_y = \sigma_{yL(f)} \; S \qquad \ldots (1)$$

The stresses used are the average tensile and compression coupon stresses for the flange. For use in preliminary design calculations, the plastic moment, M_p, may be calculated as

$$M_p = \sigma_y Z \qquad \ldots (2)$$

using the assumed stress distribution in Fig 7b. However, for theoretical calculations, a more accurate value may be calculated by considering the difference in yield strength of the flange and web. (Fig 7c) We then obtain

$$M_p = \sigma_{yL(f)} (Z-Z_2) + \sigma_{yL(w)} Z_2 \qquad \ldots (3)$$

where Z_2 is the plastic modulus of the beam web.

10. CALCULATIONS CONSIDERING KNEE AS A STRUCTURE

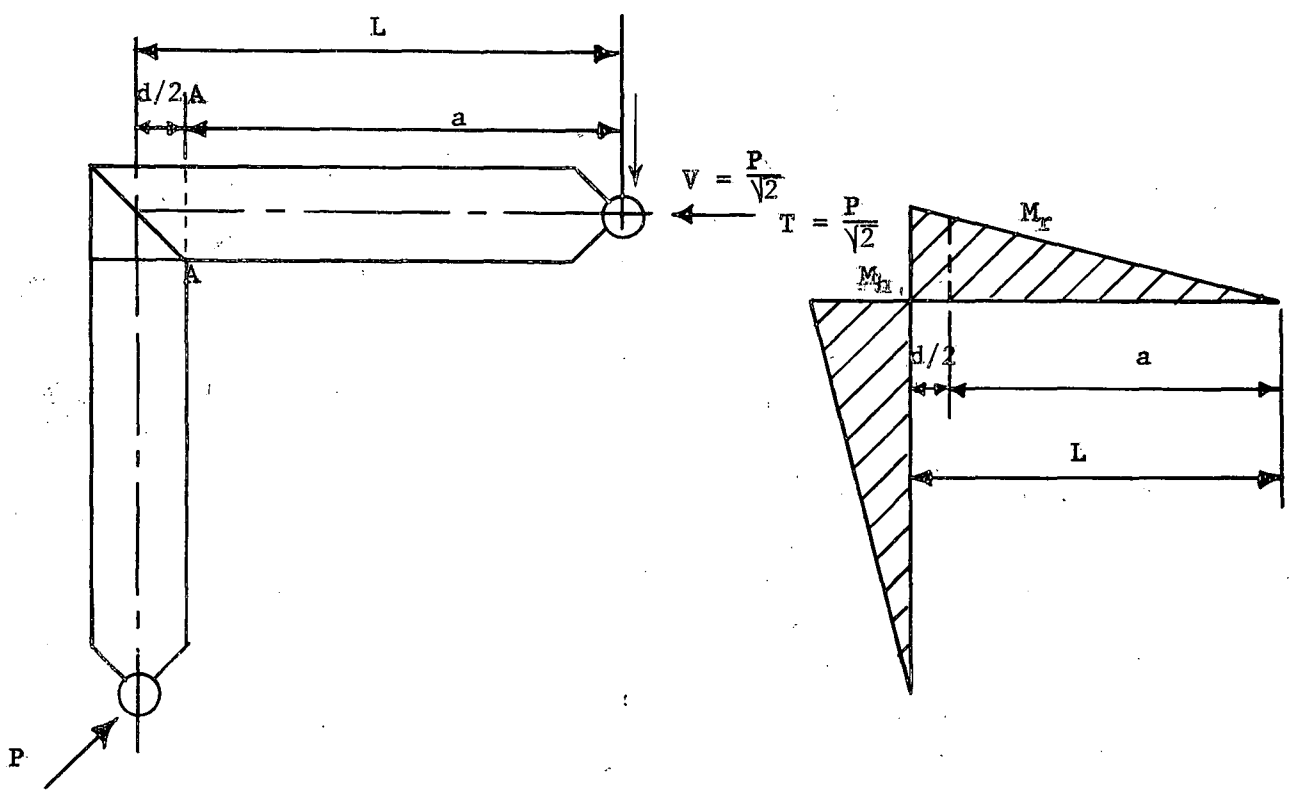

Fig 8

Considering the knee as a structure (Fig 8) the forces and stresses are of interest at two cross sections, first at the edge of the rolled section, distance "a" from the load point, and second at the haunch point, distance "L" from the load point. The loads P may be broken into axial

and transverse components equal to 0.707P.

In the calculations made for these connections, it is assumed that the connection will be made strong enough and stiff enough so that no inelastic deformation occurs within the knee in order that plastic hinges will form at the end of the rolled section. The moment at the intersection of beam and column center lines will then be slightly larger than M_p.

11. FLEXURAL YIELD MOMENT

When the extreme fibres of the compression flange just reaches its yield point at the intersection of girder and column (section AA, Fig 8), the stress due to the combined axial load plus bending is:

$$\sigma_{yL}(f) = \frac{\sqrt{2}}{2}\,\frac{P_y\,a}{S} + \frac{\sqrt{2}}{2}\,\frac{P_y}{A} \qquad \sigma = \frac{Pec}{I} + \frac{P}{A}$$

Thus:

$$P_y = \frac{\sqrt{2}\;\sigma_{yL}(f)}{\left(\frac{a}{S} + \frac{1}{A}\right)} \qquad \ldots (4)$$

where P_y is the load when yield stress is first reached in the extreme fibers of the rolled section.

The moment at the end of the rolled section at this load is

$$M_r(y) = \frac{\sqrt{2}}{2}\,P_y\,a. \qquad \ldots (5)$$

The moment at the haunch is:

$$M_h(y) = \frac{\sqrt{2}}{2}\,P_y\,L \qquad \ldots (6)$$

12. MODIFICATION OF PLASTIC MOMENT DUE TO AXIAL LOAD

At full plastification of the cross section at the edge of the

rolled section, there will be some reduction of the plastic moment due to axial load.[6] The following is an analysis to determine the extent of this modification upon the full plastic moment.

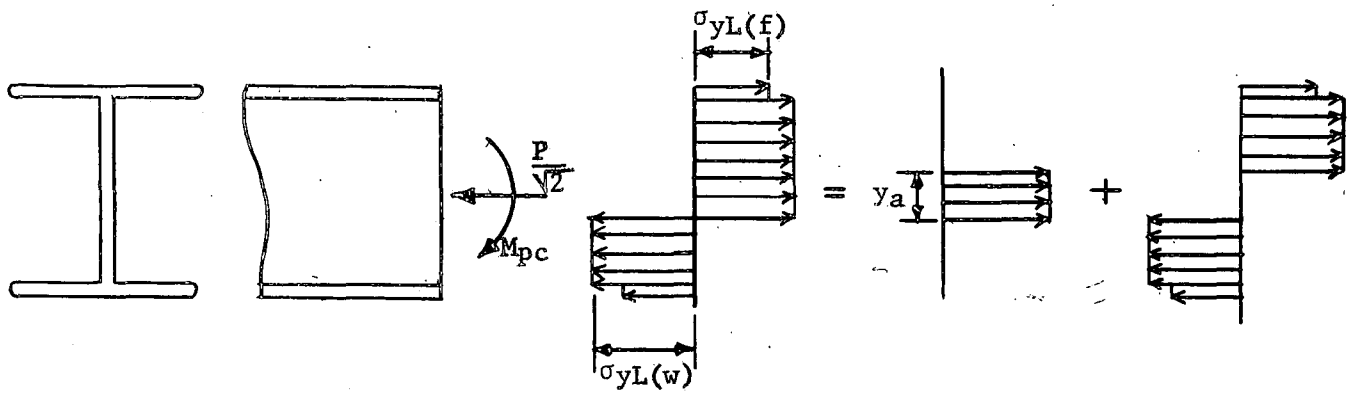

Fig 9

In the assumed stress distribution, there is yield stress across the full cross section. The axial thrust is resisted by a portion of these stresses. Assuming the axial thrust to be carried by a small area of the web near the centroid of the section, (Fig 9) this area can be calculated to be:

$$A_a = \frac{\frac{\sqrt{2}}{2} P}{\sigma_{yL(w)}} = w\, y_a \qquad \ldots (7)$$

The bending moment must be carried by the remaining portion of the cross section. From the theoretical plastic moment must be subtracted the bending resistance of the area carrying the axial force.

$$Z_a = \frac{w\, y_a^2}{4} \qquad \ldots (8)$$

$$M_{pc} = M_p - \sigma_{yL(w)}\, Z_a \qquad \ldots (9)$$

The reduced plastic moment may be calculated by assuming a value for P on the basis of full plastic moment at the end of the rolled section and calculating the reduced plastic moment resulting from this. Then

by statics, the load P to cause this moment is calculated. If this is not the same as the assumed load, a new assumption is made and the process repeated. Two trials will reduce the error to a negligible amount in most cases.

At the ultimate load, the moment at the rolled section is M_{pc}, and the moment at the haunch is $M_{h(p)} = M_{pc}\ L/a$.

The values of the theoretical moments for all the connections tested are shown in Table 3. A comparison between the values as computed from Handbook properties and those as measured are shown.

The moments indicated in the Table are arrived at in the following manner: The yield moment is obtained from Equation 1. The moment allowed by the AISC for elastic design is obtained by modifying equation 5 by the factor 20/33. Equation 6 gives the value of the haunch moment at yield. The moment at the end of rolled section is obtained from equation (5). The full plastic moment is given by equation (2). The modified plastic moment M_{pc} is given by equation (9). We can then obtain the ultimate moment at the haunch $M_{h(p)}$ by increasing the modified plastic moment by the factor L/a.

Table 4 shows the computed theoretical loads. These loads are found as indicated below. The maximum load allowed by the AISC can be found by substituting the allowable fiber stress of 20 ksi for $\sigma_{yL(f)}$ in equation 4. The yield load is given by equation 4 and the ultimate load can be found from equation 9.

13. SHEAR STRESS IN KNEE

In an earlier report[1], an equation was developed for the shear

stress up to the elastic limit in a square knee without web reinforcement

$$\tau = \frac{M_{hy}}{wd^2} \left(1 - \frac{d}{L} \right) \qquad \ldots (10)$$

The web yields when the shear stress exceeds $\tau_y = 0.578\ \sigma_y$. Investigation of all the sections to be tested showed that the webs would yield in shear at a moment lower than the flexure yield moment. Therefore, additional reinforcement in the form of diagonal stiffeners or doubler plates is required.

Expressions for the required reinforcement were developed in ref (1). The required web thickness is given by the equation,

$$w_r = 1.75\ S/d^2 \qquad \ldots (11)$$

If the web thickness is less than this, either the thickness should be increased to this thickness by doubler plates or diagonal stiffeners whose thickness is given by,

$$t_s = \frac{\sqrt{2}}{b} \left(\frac{S}{d} - \frac{wd}{\sqrt{3}} \right) \qquad \ldots (12)$$

These required stiffeners were calculated for all the knees. However, the actual thickness used was equal to the nominal flange thickness which in every case was greater than the minimum required stiffener.

The shear stress in a knee with a diagonal stiffener may be calculated from the equations developed in reference 7. (See Appendix B)

$$\tau = \gamma G = K_3 \frac{M_h}{d} (1 - d/L)\ G \qquad \ldots (13)$$

where

$$K_3 = \frac{1}{wGd + \frac{tsbs\ E}{2\sqrt{2}}} \qquad \ldots (14)$$

The critical web shear stress for buckling without diagonal stiffeners may be calculated from the equation:[8]

$$\tau_{cr} = K_s \frac{\pi^2 E}{12 (1-\mu^2)} (w/d)^2 \qquad \ldots (15)$$

where,

K_s = 14.48 for fixed edges

K_s = 9.34 for simply-supported edges

Since the haunch portion of the knee is assumed to remain elastic with the diagonal stiffener, this formula gives an indication of the shear stress which is required for elastic web buckling to occur. Table 5 shows the theoretical shearing stresses and the required web reinforcement as obtained from the above formulas.

The shear stress at yield and ultimate moments, in connections without diagonal stiffeners, is computed from equation 10. The critical web shear stress for buckling is found from Equation (15). The shear stress in the haunch when the diagonal stiffener is present was obtained from Equation (13). The required knee reinforcement is found from equations 11 and 12.

14. FLANGE STABILITY

Data from a program on inelastic instability has shown that flanges subjected to bending yield stresses will not buckle locally until after strain hardening strains have occurred as long as the b/t ratio is no greater than 17.[9] Of the sections considered, only the 14WF30 exceeded this (b/t = 18.52) and could be expected to exhibit local instability before strain hardening.

15. DEFORMATIONS

To determine whether the connections meet the requirements for the performance of knees in structures, it is necessary to compute the theoretical deformations that occur when yield stress is first reached in the outer fibers. The following section describes the theoretical expressions that were used in these computations.

Equations given in References (1) and (4) enable the corner rotations and deflections of the knees to be calculated.* In the elastic range the rotations and deflections for these particular knees can be obtained in the following manner:

$$\theta_{knee} = \frac{M_r}{d} \left\{ \frac{(L-d)}{(L-d/2)} \left(k_3 + \frac{1 + K_2}{E\ A_F} \right) \right\} \qquad \ldots (16)$$

where

$$K_2 = \frac{1}{1 + \frac{2\sqrt{2}\ wd\ G}{t_s\ b_s\ E}} \qquad \ldots (17)$$

$$\delta = \sqrt{2} \left\{ \frac{Mra^2}{3EI} + \frac{\theta L}{2} \right\} \qquad \ldots (18)$$

The rotation, $\theta_{2\ legs}$, due to flexure of the rolled section over lengths r of both legs is given by

$$\theta_{2\ legs} = \frac{M_{r_y}}{EI}\ r\ (2-r/a) \qquad \ldots (19)$$

Then the total rotation is given by a summation of the values determined from equations (16) and (19), or

---

* See Appendix B

$$\theta_{Ty} = \theta_{knee} + \theta_{2\ legs}$$

$$\theta_{Ty} = \frac{M_{ry}}{d}\left\{\frac{(L-d)}{(L-d/2)}\left(k_3 + \frac{1+k_2}{A_f E}\right) + \frac{rd}{EI}\ (2 - r/2)\right\} \quad \ldots (20)$$

Theoretical rotations and deflections are shown in Table 4. The values are shown for both measured and Handbook properties. These computations were obtained from Equations (16) and (18).

4. DESIGN AND FABRICATION OF KNEES

Once the members to be connected have been selected, the detailed design of the knees can commence. The connection must be proportioned so that it can transmit the forces and moments from one member to the other. The pieces must fit together, it must be possible to apply the welds, and the member must be as economical as possible with regard to welding and connection materials.

16. STIFFENING FOR THE KNEES

It would be an ideal situation if all that were required to make a connection would be welding the two members together. However, the large forces which are imposed perpendicular to the axis of one member by the action of the adjoining member, require that measures be taken to increase the resistance of the member to these perpendicular forces. Web crippling due to the effect of concentrated flange forces is prevented by vertical and diagonal stiffeners. The tendency for large deformations to occur due to shear yielding of the web in the vicinity of the intersection point of the two members is resisted by the diagonal stiffeners. The flange force of one member on the outside of the corner is carried to the web of the other member by an end plate. The factors considered in the selection of stiffener sizes are given below.

a. End Plates

End plates are used at the end of the beam web to prolong the outer flange of the column to meet the outer flange of the beam. Basically, the end plate must have the same load capacity as the flange. Two types of end plate were used, (Fig 10 and 11) depending on the

manner of transmitting the column flange force to the end plate. The selection of the type to be used is essentially a matter of economy. Where too great a lap joint is required, it is more economical to use a butt weld.

On the 14 inch and 8 inch knees, the end plate was lapped over the column flange with enough length to develop its strength with fillet welds on the end and the two sides. It was necessary to make the plate about 3/4 inch narrower than the flange width to allow room for the fillet welds. To obtain sufficient area, the plate therefore was made somewhat thicker than the flange. The length of overlap was determined by the length of fillet weld needed to develop the plate strength.

On the 24-inch, 30-inch and 36-inch knees, it was found that a lap joint would necessitate the use of extremely long end plates in order to develop the strength of the plate by fillet welds. (Table 6) Therefore, the connection of the end plate to the column flange was designed for a single bevel butt weld. In this case the plate was made the same width and thickness as the flanges. The plate was fastened to the beam with fillet welds along the web and inside of the flanges and along the end of the outer flange.

b. Diagonal Stiffeners

An equation given in Reference (1) suggests a value for the minimum required diagonal stiffener for a square knee.

$$ts = \frac{\sqrt{2}}{b_s}\left(\frac{S}{d} - \frac{wd}{\sqrt{3}}\right) \qquad \ldots (12)$$

where

$$w_r = 1.75\ S/d^2 \qquad \ldots (11)$$

This value was calculated for all specimens, but the size actually used was the nominal flange thickness which was bout twice the required value.

c. Half Depth Vertical Stiffeners

Vertical stiffeners were considered desirable in the beam at the end of the column inner flange to distribute the column flange force to the beam web and stiffen the beam web against crippling. Earlier tests had shown no particular improvement in behavior of full depth stiffeners over half depth stiffeners so half depth stiffeners were selected. Since the force in the stiffener would all theoretically be carried into the web by the welds by the time it reached the far end of the vertical stiffener, the stiffener could be tapered down to zero width at the end. However, the actual shape used is shown in Fig 1.

A typical design of one connection is shown in Appendix A. This indicates how the component parts of the knee were chosen once the sizes of members were known.

17. DESIGN OF WELDS

Welds serve as a means of uniting the two pieces of metal joined. The size of the welds must be sufficient to transmit the forces from one member to the other. The type of weld used depends on the shape of the members at the point they are to be joined, the amount of preparation of surfaces required before welding, the amount of weld metal to be deposited, and the ease with which a particular type of weld can be placed in the possible welding positions for that weld. A weld must be designed so that it is possible to be applied, and should be designed so that, by use of the proper welding proceedures,

distortion of the weldment can be minimized.[10]

The connections used in this program were designed with the intent that they should be satisfactory for either opening corner or closing corner load conditions. This meant that certain of the welds were required for only one of the load cases since in some cases load could have been carried to a stiffener by bearing alone.

In the design of welds for connections proportioned to carry plastic moments, stresses at or lower than the yield strength of the weld metal can be tolerated at the maximum load. In butt welds the forces are carried in compression or tension, and are limited by the tensile or compressive resistance of the base metal or weld metal, depending on which is least. This is taken as 33 ksi in plastic design. In fillet welds, the critical stress is the shear stress on the minimum throat area. The limiting shear yield stress is about 57.8% of the tensile or compressive yield stress. For plastic design purposes, however, the limiting stress assumed is 22.4 ksi which is 33/20 of 13.6 ksi, the allowable shear stress for elastic design. This procedure was followed in order that the same overload factor which was applied to the normal stresses could be applied to the shear stresses. A brief description of how these principles were used in the design of the test specimens follows.

a. Column Web Fillet Welds to Beam Flange

The column web fillet welds (see Fig 10) were designed to develop the combined tensile forces of bending and the most severe axial load component in the web and the shear force from the transverse component of load. This is the only weld which is larger for plastic

design than it is for elastic design when the same over load factor is used. The reason for this is that in elastic design the maximum stress occurs only at the ends of the fillet weld, while in plastic design the maximum stress is uniform all along the length of the weld. The weld size was found from the expression

$$D = \frac{\text{Force per inch}}{0.707 \times 22{,}400} \qquad \ldots (21)$$

where Force per inch is the resultant vector of the tensile force per inch of depth of web and the shear force per inch of length of weld.

For the large size connections, the use of a fillet weld required a large volume of weld metal and as many as 13 passes in welding, but in this case it was preferred as against the preparation of the web for a butt weld.

b. Weld to Connect Inner Flange of Column to Inner Flange of Beam

These welds were designed first as fillet welds which would develop the plastic flange force when the corner was subjected to an opening corner load condition. The results obtained were satisfactory for the 8B13 and 14WF30, (see Table 6) but in the case of the large size members (24WF100, 30WF108, and 36WF230) the size fillet weld required was so large that it was more feasible to use butt welds for these larger members. Fig 10 shows a typical butt weld that is to be placed at the veentrant corner. The size fillet weld required was found from

$$D = \frac{\text{Flange Force}}{0.707 \times 22{,}400\ (2b-w)} \qquad \ldots (22)$$

where the flange force is $\sigma_{yLf} A_f$

c. End Plate to Beam Web

These welds were designed as fillet welds to transmit the plastic flange force from the flange of the column into the web of the beam by shear. (Fig 10 and 11) The size fillet weld required was obtained from the following expression.

$$D = \frac{\text{Flange Force}}{0.707 \times 22{,}400 \times 2\ (d-2t)} \qquad \ldots (23)$$

Since most wide-flange shapes do not have sufficient web thickness to resist the full plastic flange force in shear, these welds need only develop the web shear strength. The unbalance in the flange force is then transmitted to the diagonal stiffener. These welds will be somewhat smaller when this procedure is followed.

d. End Plate - Lap Joint to Flange of the Column

For the small size sections (8B13 and 14WF30) a lap joint was used to transfer the plastic flange force from the column to the end plate and then into the web of the beam. (see Fig 11) The lengths required were reasonable and it was feasible to use a lap joint to develop the flange force. But in the larger section the length of lap joint required to develop the plastic flange force was uneconomical to use and a butt weld was used instead between the end of the column flange and the end of the end plate, (Fig 10) since the section through the throat need be only the thickness of the flange. The length lap joint needed was found from

$$L = \frac{\text{Area of Weld}}{0.707D} \qquad \ldots (24)$$

$$\text{where Area of Weld} = \frac{\text{Flange Force}}{22{,}400} \qquad \ldots (25)$$

e. Diagonal Stiffener to the Flanges at the Corner

The force in the diagonal stiffener is found from the equation

$$(\sigma_{y_{L(f)}} K_2 \, bt \sqrt{2}) = F_s. \qquad \ldots (26)$$

where K_2 is given by (Eq 17). The size fillet welds needed at the ends of the stiffeners to attach them to the flanges, end plate, and vertical stiffener (see Fig 10) is then computed using a 45° fillet at that point or

$$D = \frac{\text{Diagonal Stiffener Force}}{22{,}400 \times 2(b-w) \cos 221/2^{\circ}} \qquad \ldots (27)$$

Since the theoretical force carried to the diagonal stiffener by the fillet welds at its ends would shorten (or lengthen) the stiffener the same amount as shortening of the beam web along the same diagonal line due to shear, only a minimum fillet weld is required between stiffener and web plate. This provides stiffening against buckling of the web and stiffeners. The minimum fillet weld provisions of the AWS building code were followed.

f. Fillet Welds for the Half-depth Vertical Stiffeners

The assumptions made are (1) that the maximum possible flange force must be borne by the beam web and the half-depth stiffeners, (2) the concentrated load is distributed to the web on planes bounded by 45° angles from the point of application of the load. (Fig 12)

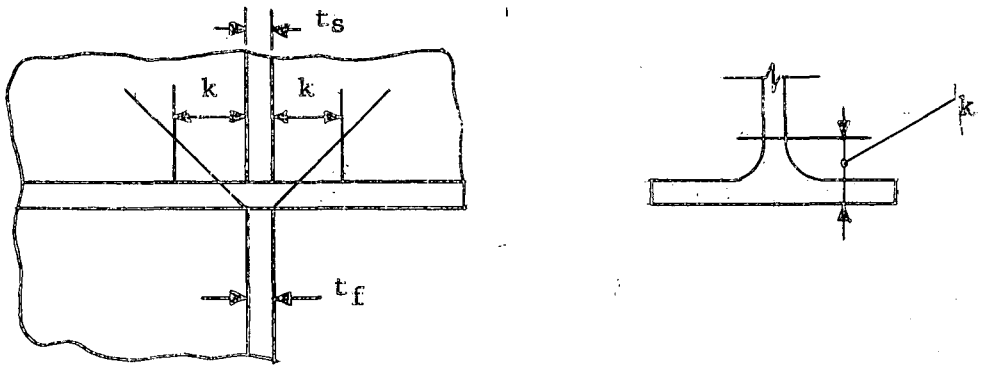

Fig 12

The force carried by the web of the beam is then

$$\sigma_y L(w) \ (t_f + 2k) \ w. \qquad \ldots (28)$$

The force in the vertical stiffener is the difference of the maximum possible flange force and the force carried by the web. The size of the fillet welds is then computed using an effective length of weld of (d/2 - k)

$$D = \frac{\text{Force in half-depth stiffener}}{4 \times 0.707 \times 22{,}400 \ (d/2 - k)} \qquad \ldots (29)$$

The weld connecting the end of the half-depth vertical stiffener to the beam flange was arbitrarily made similar to the weld connecting the column flange to the beam flange. For a connection designed to take only a compression type load, it would be sufficient to provide a minimum fillet weld. However, for a tension type loading, the flange force is assumed to be transferred to the half depth stiffener.

18. A COMPARISON BETWEEN PLASTIC AND ELASTIC DESIGN OF WELDS

In proportioning welds for these A-7 steel specimens, the design forces are based on the yield stress (σ_y) of the base metal (which is taken as 33 ksi) and the yield stress of the weld metal is obtained by increasing the allowable stresses by the factor 33/20 x 20 ksi for butt weld and 33/20 x 13.6 ksi for fillet welds.

If the design of weld for a particular test specimen is based on the measured cross section and strength of section as determined by coupons while using 33 ksi for butt welds and 22.4 ksi for fillet welds, it is found that for sections having a yield stress greater than 33 ksi, larger welds are needed for plastic design than are needed for

elastic design. This is due to the increased strength in plastic design due to the higher yield level.

However, in practice one is not allowed this increase due to the higher yield. And when the same factor of safety is used for both elastic and plastic design, the only weld which is larger by plastic design is the column web fillet weld to the beam flange.

Table 6 shows a comparison between elastic and plastic design for size of fillet welds needed based on handbook properties. The size weld actually used is also shown.

A comparison between plastic and elastic design of the welds for the 24WF100 connection is shown in Appendix A.

19. WELDING SEQUENCE

Careful attention to the welding sequence is important in any welding job. For economy's sake, it is best to try to perform as much of the welding as possible in the flat or horizontal positions, restricting the use of other positions when necessary to small welds. In doing this it is also desirable to have as little handling of the material being welded as possible. Welding sequence is also important from the standpoint of induced stresses and distortion. By the use of proper procedures These may be controlled to a reasonable degree.

The sequence used for welding the larger connections tested are as follows:

The component parts of the connection were placed so that as much welding as was possible could be done making downhand passes. This

required turning and rolling the members as the connection was fabricated. Also a certain sequence was used when welding component parts of the knee to minimize the distortion that could occur thru welding.

Pieces of the connection were first tack-welded to keep alinement and then the welding was completed with a block sequence by welding alternately as indicated in Fig 10 so that the distortion effects of shrinkage would be at a minimum and thermal cracks in welds avoided.

The following is an example of how the test connections were positioned and welded to comply with the above procedures.

The beam was first set upright on the end plate and short downhand fillets placed as indicated in Fig 10 along the web. The fillets were also placed at intersections of the flanges and plate. The beam was then placed on the floor in its normal position and the corner weld placed, as indicated in Fig 10 section a-a.

The vertical half depth stiffeners were positioned with the beam in its normal position and then vertical fillet welds were placed to fasten the vertical stiffeners to the beam web on either side. Root passes for the single bevel butt welds were placed from inside the stiffeners. After chipping out all weld metal form the grooves, the single-bevel butt welds were made in the horizontal position.

The beam was then rolled on its side, the diagonal stiffener was placed, and downhand fillet welds were made along the stiffener and beam web, with welds placed alternately in short sections as indicated in Fig 10. The beam was rolled and the other stiffener was welded. Forty-five degree vertical fillet welds were then made at each end of

the diagonal stiffener to connect it to the beam flanges, end plate and vertical half depth stiffener. The beam was rolled back and the procedure repeated for the other side.

The beam was next laid on its top flange and the column set in place on the bottom flange. The connection of the column web to the beam flange was made by means of fillet welds made in the horizontal position using a block sequence as shown in Fig 10. Fillet welds were placed at the inside of the column flanges to serve as a root pass for the single-bevel groove welds connecting the column flanges to the beam flanges. After chipping all weld metal from the bevelled groove, the butt welds were placed outside the groove, the butt welds were placed outside the flanges, (Fig 10-B and 10-C) welding first the center third and then the two outer thirds by the back-step method.

The above procedure was typical for the 24WF100, 30WF108, and the 36WF230 connections. For the 8B13 and 14WF30 the procedure was slightly different due to the fact that a lap joint was made to develop the strength at the end plate instead of the butt weld used for the larger size members. Also fillet welds were used for the column flange connection instead of butt welds as is indicated on Fig 11.

Since the members being connected were small and could be handled with ease the welds were applied in the block sequence shown in Fig 11. Opposite welds were applied in succession by turning the connection after each short weld.

It was not felt necessary to use a preheat or low hydrogen electrodes on any of the connections fabricated. The recommendations given in reference (4) were followed in determining the welding procedure.

"For plates and shapes in all thicknesses up to and including 1, use A7 steel without preheat or low hydrogen electrodes. For plates and shapes with thicknesses over 1" and up to 2", A-7 steel can be used without preheating or using low hydrogen electrodes, if the mill report shows the carbon equivalent to be less than 0.43%".[4]

The only shape used in the fabricated connection which had a thickness greater than 1" was the 36WF230. The mill report of this shape showed it to contain 0.19%C and 0.70%M. This gave a carbon equivalent of 0.31%, so it was considered unnecessary to use a preheat or low hydrogen electrode.

Table 7 shows the chemical properties of the rolled shapes used. These were obtained from the metallurgical report of physical and chemical tests. The type of electrodes used for welding were E6012 (3/16,5/32) for poor fitup in all positions and E6020 (1/4, 3/16) for horizontal fillet and flat positions.

5. RESULTS OF TESTS

The results of the experimental investigation are reported below.

20. MOMENT-DEFLECTION RESULTS

In Fig 13 the curves of non-dimensionalized values of $\frac{M_h}{M_y}$ vs $\frac{\delta}{\delta_y}$ are given for all the connections tested in this series. The values of M_y and δ_y are computed from the theoretical considerations as presented earlier in this report, using coupon data and actual cross section measurements to determine their value.

The haunch moment, M_h, is computed at the intersection of the neutral lines of the adjoining members of the connection. (Fig 8) In all curves, the moment has been corrected for the measured increase in moment arm due to the deflection between end pins. The deflection between end pins of the connections was measured by a gage as indicated in Fig 5.

The predicted values for M_p, M_{hp} and M_y of each connection tested fall within the bounds indicated along the ordinate.

The load at which yield occurred in the knee web due to the shear force is indicated by the symbol "S" in Fig 14. Compressive yield of the flanges is indicated by the symbol"Y". The points at which yield occurred were obtained by observing the flaking of mill scale as revealed by the whitewash coating. The loads at which local buckling occurred are indicated in Fig 14 by the symbol "L". This point was

obtained by the buckling gages that were employed. The theoretical curves were obtained from equations 6 and 13. These values are not shown for the 30WF108. Since this connection was tested as a short duration demonstration, a complete set of data was not taken.

Fig 15 shows the behavior of the 36WF230 corner connection. The condition of the connection at different stages of the test is indicated by photographs in the upper portion of the Figure. The corresponding point is located on the non-dimensional curve of moment versus deflection.

21. MOMENT-ROTATION RESULTS

In Fig 16 the non-dimensionalized curves of $\frac{M_h}{M_y}$ vs $\frac{\theta_T}{\theta_{T_y}}$ are shown. θ_T is the total rotation experienced by the knee portion of the connection in the vicinity of the junction of column and beam as shown by the sketch in Fig 16. This rotation was measured by rotation indicators using dial gauges as shown in Fig 6. Theoretical values for M_p, $M_{h(y)}$, $M_{h(p)}$ and M_{all} for the connections tested are indicated along the ordinate and fall within the spread indicated.

Separate M-rotation curves for the "elastic" range and for the first portion of the plastic range are shown in Fig 17. It also indicates the points at which shear yield in the web, compressive yield of the flange and local buckling of the connection occurred.

The theoretical curve represented by the dashed line was obtained from equations (6) and (16).

The above figures indicate that the connections were able to rotate through an adequate angle before failure.

Although shear yielding in the web of the 24WF100 began at a low ratio of M_h/M_y this had little effect on the behavior of the connection.

22. PLASTIC BUCKLING AND LATERAL SUPPORTS

Figures 18, 19, 20, and 21 are photographs showing the connections in the vicinity in which the plastic hinges formed. Yielding in the compression flange, web, and tension flange is indicated by the dark lines in the white-wash caused by flaking of mill scale.

Table 8 shows the magnitude of lateral forces that were present at certain stages of the test. These stages are indicated in the footnotes of the Table. In order to prevent buckling of the lateral support rods, they were pretensioned and maintained under tension during as much of the test as possible. The lateral forces were measured by dynamometers which were placed in the lateral support system.

Figures 18, 19, 20, and 21 show the general mode of failure for the connections. After considerable yielding, the compression flanges tended to buckle locally in a wave-like formation. As the load was increased, one side of the flange tended to buckle more which in turn forced the web to buckle and caused the failure at the connection. Local buckling of all connections occurred simultaneously with lateral buckling. This was determined by observation of the various buckling gages and careful inspection of the specimen.

Web buckling was detected with the device shown in Fig 23. The corresponding local buckling curves obtained for the 36WF230 are also shown in this Figure. Flange buckling was measured with the gage indicated on Fig 22. The local buckling curve of the beam flange of the 36WF230 connection is also shown in Fig 22.

6. DISCUSSION OF RESULTS

In the following paragraphs, the test results are discussed for each connection tested. The primary reason for this study was to determine if the results obtained for Phase I (series of tests of corner connections of one size having different design details).[1] would hold true for connections fabricated of larger rolled sections.

8B13

This connection was tested under Phase I. The connection was able to develop the strength and rigidity required. It was capable of developing the M_p-value and of carrying it through large rotations. From Figs 13 and 16 we can see that the connection was able to sustain a rather large deformation and rotation. It followed the theoretical predicted curve with reasonable accuracy until the yield moment was reached. It was only after considerable yielding that plastic local buckling started in the flanges. This was accompanied by a simultaneous lateral buckling which eventually caused failure.

As can be seen in Fig 16 and Fig 18 the diagonal stiffener provided sufficient stiffness to prevent serious shear deformation. In Fig 18 which was taken at failure, yielding due to the shear force still occurred as can be seen by whitewash pattern. These results are given for comparison with the other connections tested.

14WF30

This was the first specimen tested in Phase II (size effect series). As observed from Fig 16, the connection was capable of developing the plastic moment and was able to carry it through a rather large rotation

before the moment started decreasing. In Fig 17 the moment-rotation curve shows that the connection started to deviate much sooner from the theoretical elastic behavior, based on coupon stress and measured cross section, than the 8B13, 24WF100, or 36WF230. In Fig 13, the moment vs deflection curve shows that the connection was capable of sustaining a deflection curve shows that the connection was capable of sustaining a deflection of approximately 7 times that predicted at theoretical yield. The first local buckle occurred shortly after general yielding and accompanied a slight drop in moment. However, the moment continued to build up even after local buckling, and the plastic moment was exceeded.

The failure of the specimen was caused by the local buckle which formed outside the knee. This occurred in an unsymmetrical manner as can be seen in Fig 19. Lateral buckling was not detected during the test of this specimen. This behavior could be expected due to the b/t ratio being greater than 17.

Since yielding results in a reduction in stiffness, lateral support is needed to develop the strength and rigidity of the connection. That it was adequate is indicated by the development of M_p and the deformation that it was able to sustain while carrying the plastic moment, without lateral buckling developing.

The whitewash pattern observed in Fig 19 indicates that some yielding takes place due to shear forces in spite of the excess web stiffening. Fig 26 shows the connection when the first shear yield lines appeared.

24WF100

As seen by Fig 16 the connection was able to sustain a rather large rotation and also develop the plastic moment of the rolled section. The shear yield in the web was observed at approximately half the value of M_h/M_y that the other connections exhibited. (Fig 17) This was possibly due to the 24WF100 having proportionally the smallest web area. Another possibility is greater residual stresses in members or possibly stress concentrations and residual stresses from welding.

In Fig 13 the moment-deflection curve is shown. It can be seen that the connection was able to withstand a rather large deformation without any weld fracture occurring.

Fig 27 shows the connection when the first shear yield lines were observed.

A well defined yield point was not observed; this is the case with most structural members as was pointed out in Reference (1).

Local buckling of the beam flange (Fig 20) was followed by an immediate increase in deformation.

The lateral support can be concluded to be adequate since the connection was able to rotate and deform through a relatively large range. This was also accompanied by an increase in plastic strength. The lateral forces present after the mechanism had formed and at the maximum moment are shown in Table 8.

30WF108

This connection was not a part of the program originally planned for the "size effect" series. However, the results obtained from

testing it as a demonstration gives an opportunity for making another comparison with the measurements taken.

It can be seen in Fig 14 that the connection followed very closely the predicted theoretical results. It was able to sustain a moment exceeding the plastic moment through a deformation of about 10 times that at the predicted theoretical yield (Fig 13). The actual rotation of the connection was somewhat less than the theoretical predicted value according to Eq 21. However, the connection was able to sustain a rotation of approximately 10 times that predicted at yield.

The reason for the apparent deviation of the 30WF108 as compared to the other connections was probably the effect of the position of the rotation indicators. The indicators were attached to the connection in the middle of the connection as shown below. (Fig 24a) Bending of the 30WF108 web would tend to misalign the rotation indicators giving an apparent change in reading greater than the actual rotation.

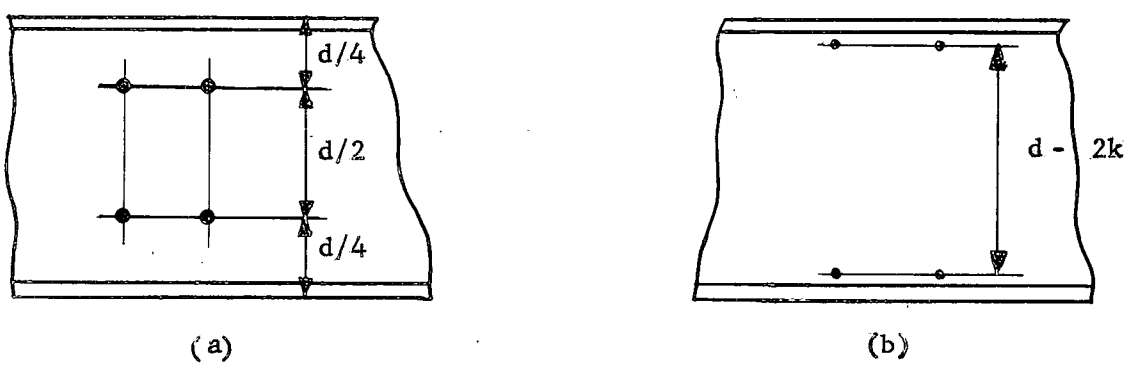

Fig 24

The other connections tested had the rotaton indicator attached to the connection very near the flanges (Fig 24b). Bending of the web

would have less effect on the indicators when placed in this manner.

No data was taken on shear yield in web, compressive yield in flange, or when local buckling first occurred.

The lateral support was more than adequate as can be seen by the large rotation and deflection that were possible while the moment was equal to or exceeding the plastic moment.

36WF230

This largest connection in the series was capable of sustaining the greatest rotation and deformation (Fig 13 and 16) while developing the plastic moment. It followed very closely the behavior of the 24WF100 for a considerable distance in both rotation and deformation. The connection was capable of withstanding a deflection approximately 13 times as great as δ_y, based on coupons and measured section. The rotation was approximately 10 times that of θ_y.

Lateral support can be assumed to have been adequate since the connection was able to sustain a larger rotation and deflection than any of the others tested. No difficulty was encountered in reaching the full computed plastic moment and exceeding it.

Local buckling (Fig 21) of the girder was symmetrical and was thus favorable to an increase in load. It was only after rather large deformation that lateral instability followed and ultimate failure of the connection was brought about.

Yielding in the knee web due to the large shear strains that occurred in the knee web as the connection deformed, caused the half-depth stiffener to be bent (Fig 25) in the direction of the end pin.

The point of shear yield in the web was very close to that of the 14WF30 and 8B13. The yield lines can be seen in Fig 28.

7. SUMMARY AND CONCLUSIONS

The following observations summarize the elastic behavior of the connections:

(1) Agreement with the theoretical moment-deflection and moment-rotation behavior in the elastic range was fair. (Fig 13 and 16) The effect of the shear yield lines which were observed at a very low load while testing the 24WF100 can be seen in Fig 13.

(2) Yielding of the web of the knee due to the shear forces occurred at a load considerably lower than the predicted flexural yield. (Fig 14 and 17)

(3) Flexural yielding of the flanges occurred at a lower load than predicted. (Fig 14 and 17) A well-defined yield point was not observed on any of the connections tested. (Fig 13 and 16) Presumably the premature yielding occurred as a result of residual stresses, shear yielding, and stress concentrations.

(4) None of the observed deviations in the elastic portion of the test had a detrimental effect on the ability of the connection to carry load or reach its M_p-value.

In the plastic range, the following general observations of the behavior of the knees were made:

(1) All connections reached the predicted plastic moment at the end of the rolled section, and exceeded it by 7.5 to 22%. This can be seen in Figs 13 and 16 which shows the predicted ultimate moment in the haunch when this occurred.

(2) Sufficient rotation was attained near maximum plastic moment after the formation of plastic hinges to have allowed redistribution of moment if the knee were part of an indeterminate structure. (Fig 16)

(3) Strain hardening occurred almost immediately after the plastic hinge moment had been reached in each case and thus allowed an increase above the moment predicted by simple plastic theory. This normally occurs in flexural members with steep moment gradient. However, the 14WF30 which did exhibit local instability before strain hardening could not sustain the increase in moment through a very large rotation or deflection. (Fig 13 and 16)

(4) After exhibiting sufficient strength and rotation capacity to meet the requirements for connections, all connections but the 14WF30 failed by lateral torsional buckling in combination with local buckling in the web and flanges. The 14WF30, which has a b/t ratio greater than 17 failed primarily due to local buckling. (Fig 19)

(5) The lateral support forces required to prevent lateral buckling until the members reach their maximum load are very small. In no case did these forces exceed more than 1 to 2% of the force that would be required to yield the main member if it were loaded axially as a stub column (Table 8).

(6) There were no weld cracks or failures, even after straining the knees much more than the amount necessary to merely reach maximum load. It was not necessary to use heat treatment or low hydrogen electrode to fabricate any of the connections.

From the results of these tests, the following conclusions can be drawn about the effect of size of rolled shape on the behavior of straight corner connections:

(1) The behavior of straight welded corner connections joining rolled wid-flange shapes is not affected by the size of member. (Figs 13 and 16)

(2) All the sizes of connections are able to develop the full plastic moment of the rolled sections joined. (Figs 18, 19, 20, and 21)

(3) The stiffness of the knees is approximately the same as was computed theoretically. It can be seen from Fig 15 that the observed rotation was only a few percent greater than predicted.

(4) Connections of large size members are able to absorb a reasonable amount of further rotation at near-maximum plastic moment provided adequate lateral support is funished to prevent premature failure of the knee. (Fig 16)

(5) The magnitude of the lateral support forces necessary to assure satisfactory strength and rotation capacity are relatively small. These forces are so small that the size of bracing members will likely be determined from slenderness considerations rather than strength (Table 8)

(6) Welds designed for a stress of 33 ksi in tension or compression and a stress of 22.4 in shear at the ultimate load of the structure have sufficient strength to allow the connection to reach the plastic hinge moment.

(7) Proper welding procedures planned to minimize distortion of

weldments along with careful inspection of the welding will assure the development of plastic hinge without premature fracture of the welds in A-7 structural steel.

In general the increased size of the rolled members joined has no adverse effect on the overall behavior of rigid knees, and places no restrictions on their design.

8. ACKNOWLEDGEMENTS

This work has been carried out at Lehigh University in the Fritz Engineering Laboratory. William J. Eney is Director of the Laboratory and Head of the Department of Civil Engineering. The work was done as part of a larger program on Welded Continuous Frames and Their Components sponsored jointly by the Welding Research Council and the U. S. Navy. Technical guidance for this project is furnished by the Lehigh Project Subcommittee of the Structural Steel Committee, Welding Research Council. T. R. Higgins is chairman of the Lehigh Project Subcommittee.

The authors wish to express their appreciation for the helpful suggestions of the Lehigh Project Subcommittee in the design and fabrication of the specimens, and especially to Messrs. J. O. Jackson, Jonathan Jones, C. L. Kreidler, H. W. Lawson, and N. M. Newmark who furnished detailed sketches and comments on the specimens.

Specimens were fabricated in the laboratory shop and erected in the testing machine by Kenneth R. Harpel, foreman, and the laboratory staff of machinists and technicians. Instrumentation was installed by I. J. Taylor, instruments associate.

Thanks are also extended to S. J. Errera, Y. Fujita, A. T. Gozum, S. Niimoto, P. C. Paris, C. G. Schilling, A. N. Sherbourne, and M. W. White who helped perform the tests, and to Dr. L. S. Beedle who directed the project and reviewed the manuscript.

9. REFERENCES

Topractsoglou, A. A.
Beedle, Lynn S.
Johnston, Bruce G.
"CONNECTIONS FOR WELDED CONTINUOUS PORTAL FRAMES", The Welding Journal Research Supp. Vol 30, p 359-s to 384s, 397s to 405s, Vol 31, p 543-s to 560-s, July and August 1951, November, 1952.

Beedle, Lynn S.
Huber, Alfons W.
"RESIDUAL STRESS AND THE COMPRESSIVE STRENGTH OF STEEL", The Welding Journal Research Supplement, Vol 30, p. 582s-614s, December 1954.

American Institute of Steel Construction
"STEEL CONSTRUCTION", American Institute of Steel Construction, 101 Park Avenue, New York 17, New York, 1952.

Greenberg, Simon A.
"STEEL FOR WELDED BRIDGES AND BUILDINGS", American Society of Civil Engineers, Proc. Paper No. 344, ASCE November, 1953.

Ruzek, J. M.
Knudsen, K. E.
Johnston, E. R.
Beedle, L. S.
"WELDED PORTAL FRAMES TESTED TO COLLAPSE", Proceedings Society for Experimental Stress Analysis, Vol XI, No 1, May 1952

Beedle, L. S.
Thurlimann, B.
Ketter, R. L.
"PLASTIC DESIGN IN STRUCTURAL STEEL", American Institute of Steel Construction, 101 Park Avenue, New York 17, New York

Beedle, Lynn S.
"ELASTIC, PLASTIC, AND COLLAPSE CHARACTERISTICS OF STRUCTURAL WELDED CONNECTIONS" Dissertation, Lehigh University, 1952.

Bleich, Frederick
"THE BUCKLING STRENGTH OF METAL STRUCTURES", McGraw-Hill Book Co., 1st ed. (1952.

Haaijer, G.
Thurlimann, B.
"ON INELASTIC BUCKLING IN STEEL", F. L. Report 205E.9, Lehigh University, May 1957

The Lincoln Electric Company
"PROCEDURE HANDBOOK OF ARC WELDING DESIGN AND PRACTICE", The Lincoln Electric Co., Cleveland 1, Ohio

Timoshenko, Stephen
"THE THEORY OF ELASTICITY", McGraw-Hill Book Company Inc., New York (1936)

10. NOMENCLATURE AND TERMINOLOGY

A = Area of Section

A_a = Area assumed to carry axial thrust

a = Distance between point of inflection and junction of rolled beam and connection.

A_w = Area of web

A_f = Area of one flange

A_s = Equivalent stiffener Area

b = Flange width

b_s = Total width of stiffener

D = Size of fillet weld

d = Depth of section

E = Young's modulus of elasticity

F = Flange force

F_s = Force in stiffener

G = Shearing modulus of elasticity

I = Moment of inertia of section

L = Distance between the point of inflection and the haunch point.

M_a = Bending moment of area carrying the axial load = $\sigma_y Z_a$

M_h = "Haunch" moment subscript y refers to moment at yield; subscript p refers to moment at reduced plastic moment.

M_p = "Hinge" value of full plastic moment; the ultimate moment that can be reached at a section according to the simple plastic theory $\sigma_y Z$

M_{pc} = Reduced plastic moment due to axial load

M_r = Moment in a connection at junction of rolled beam and connection

M_y = Moment at which yield point stress is reached in the rolled section $\sigma_{yL(f)}$ S

P = Load on knee

P_y = Load when yield stress is first reached in the extreme fibers of rolled section

r = Distance from end of knee to point of rotation measurement

S = Section modulus of beam

t = Flange thickness

t_s = Stiffener thickness

w = Web thickness

w_r = Required web thickness

V = Transverse shear force

y_a = Depth of web that carries axial force

Z = Plastic modulus; the combined statical moments of the cross-sectional areas above and below the neutral axis. Subscript "a" refers to area carrying axial force, subscript "2" refers to plastic modulus of web.

β = Rotation in connection due to bending

γ = Rotation in connection due to shear

δ = Deflection

θ = Rotation (subscript "T" refers to total rotation within a rotation indicator "y" refers to rotation of knee at yield)

σ = Direct stress (bending): σ_{yL} = lower yield - point stress; subscripts "f" and "w" refer to flange and web.

τ = Shear stress

ϕ = Average unit rotation

μ = Poisson's ratio

Haunch point:	The intersection of the extended center lines of girder and column.
Rotation capacity:	The ability of a structural member to rotate under near-constant moment.
Yield Lines:	Flaking of mill scale following the formation of Luder's lines as revealed by whitewash.
Plastification:	The development of full plastic yield of the cross-section.
Plastic Hinge Moment:	The ultimate moment that can be reached at a section according to simple plastic theory.
Ultimate Load:	Maximum possible load that the structure can sustain.

11. APPENDIX A

Sample calculations from the analysis of 24WF100 connection to determine stress, theoretical deflections, and welds required using the equations and concepts given in sections 9 through 12, and the handbook properties given in Table 2.

A. STRESSES AND DEFLECTIONS

The connection has the following assumed proportions. (Fig A.1)

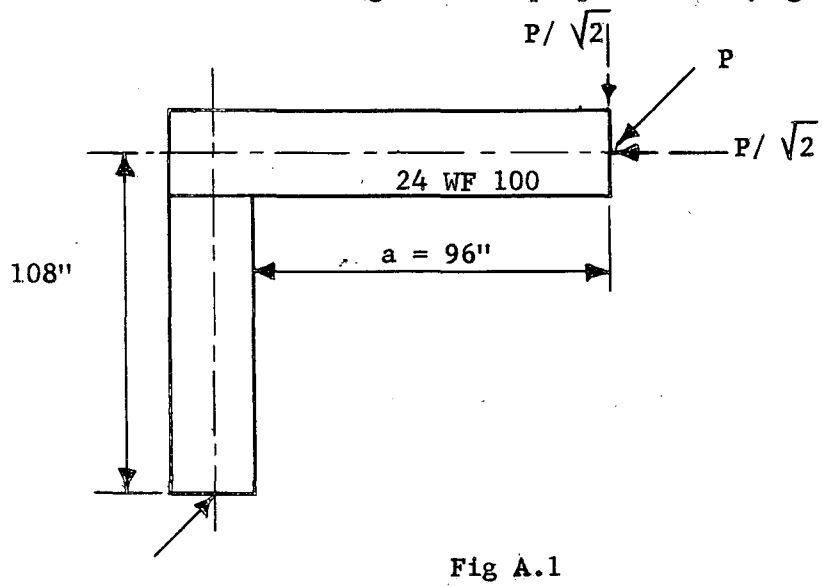

Fig A.1

1) Yield Moment and Axial Force

The yield moment is found from Eq (1):

$$M_y = \sigma_y S$$
$$= 33 \times 248.9$$
$$= 8{,}210 \text{ in-k}$$

The plastic moment of the section is found from Eq (2):

$$M_p = \sigma_y Z$$
$$= 33 \times 278.3$$
$$= 9{,}170 \text{ in-k}$$

To determine the allowable axial force at first yield, the combined bending and axial force formula is used

$$\sigma = \frac{P_y}{A} + \frac{M}{S}$$

Therefore:

$$33 = \frac{P_y}{\sqrt{2}} \left\{ \frac{1}{A} + \frac{a}{S} \right\}$$

Hence from Eq (4):

$$P_y = \frac{33\sqrt{2}}{\frac{1}{29.43} + \frac{96}{248.9}}$$

$$= 111.4 \text{ kips}$$

The moment at the haunch can then be determined from Eq (6) as

$$M_{hy} = \frac{P_y}{\sqrt{2}} (a + d/2)$$

$$= \frac{111.4}{\sqrt{2}} \times 108$$

$$= 8{,}500 \text{ in-k}$$

2) Ultimate Axial Force

The ultimate axial load is found by determining the interaction between the plastic moment, M_p, of the section and the reduction due to axial load. An ultimate value of P is assumed from which the depth of web, y_a, (Fig A.2) required to support the axial load is found.

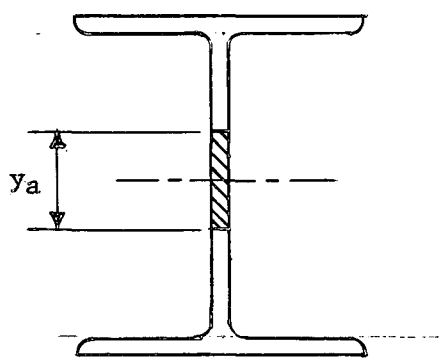

Fig A.2

An an example assume $P = 135^k$; then from Eq (7):

$$y_a = \frac{P}{\sqrt{2}\sigma_y W}$$

$$= \frac{135}{\sqrt{2} \times 33 \times 0.468}$$

$$= 6.18 \text{ inches}$$

The plastic modulus of this area is obtained from Eq (8);

$$Z_a = \frac{w\ y_a^2}{4}$$

Therefore the bending moment of the area carrying the axial load

$$M_a = \sigma_y Z_a$$

$$= \frac{33 \times 0.468 \times 6.18^2}{4}$$

$$= 144.3 \text{ in-k}$$

Hence: Eq (9):

$$M_{pc} = M_p - M_a$$

$$= 9{,}170 - 144$$

$$= 9{,}026 \text{ in-k}$$

From statics

$$P_u = \frac{\sqrt{2}\ M_{pc}}{a}$$

$$= \frac{\sqrt{2} \times 9{,}026}{96}$$

$$= 133 \text{ kips}$$

Next assuming P_u = 133 kips and repeating the process gives from statics:

$$P_u = 133 \text{ k}$$

3) Shear Stress Without Web Reinforcement

From Eq (10):

$$\tau_y = \frac{M_{h_y}}{wd^2}\ (1 - d/L)$$

$$= \frac{8500}{0.468 \times 24^2}\ (1 - 24/108)$$

$$= 24.25 \text{ ksi}$$

This exceeds 0.578 σ_y therefore additional reinforcement is required. The shear stress at the ultimate load is

$$\tau_u = \frac{M_{h_p}}{wd^2}\ (1-d/L)$$

where

$$M_{h_p} = \frac{P_u}{2}\ (a + d/2)$$

Hence:

$$\tau_u = \frac{10,150}{0.468 \times 24^2} (1 - 24/108)$$

Giving:

$$\tau_u = 29.2 \text{ ksi}$$

4) Required Reinforcement

The required web thickness from Eq (11)

$$w_r = \frac{\sqrt{3}S}{d^2}$$

$$= \frac{\sqrt{3} \times 248.9}{24^2}$$

Giving: $w_r = 0.749$ inches

The thickness of the diagonal stiffeners is then (Eq 12)

$$t_s = \frac{\sqrt{2}}{b} \left(\frac{S}{d} - \frac{wd}{\sqrt{3}}\right)$$

$$t_s = \frac{\sqrt{2}}{12} \left\{ \frac{248.9}{24} - \frac{(0.468)}{\sqrt{3}} (24) \right\}$$

$$= 0.457 \text{ inches}$$

5) Shearing Stress at Ultimate Load With Diagonal Stiffener

From Eq (13)

$$\tau = K_3 \frac{M_{h_p}}{d} (1 - d/L) G$$

and Eq (14)

$$K_3 = \frac{1}{wGd + \frac{t_s b_s E}{2\sqrt{2}}}$$

$$= \frac{1}{0.468 \times 11.5 \times 10^3 \times 24 + \frac{0.548 \times 11.53 \times 30 \times 10^3}{2\sqrt{2}}}$$

$$= 0.453 \times 10^{-5}/\text{kip}$$

Hence:

$$\tau = \frac{0.453}{24} \times 10^{-5} \times 10,150 (1-24/108) 11.5 \times 10^3$$

$$= 17.15 \text{ ksi}$$

6) Rotation of the Knee at Yield

The rotation at yield is given by Eq (16)

$$\theta_y = \frac{M_{r_y}}{d} \frac{(L-d)}{(L-d/2)} \left\{ K_3 + \frac{(1 + K_2)}{E \; A_f} \right\}$$

where (Eq 5)

$$M_{r_y} = P_y \frac{a}{\sqrt{2}}$$

$$= \frac{111.4 \times 96}{\sqrt{2}}$$

$$= 7{,}580 \text{ in-k}$$

Using Eq (17)

$$K_2 = \frac{1}{1 + \frac{2\sqrt{2}\, wdG}{t_s \; b_s \; E}}$$

$$= \frac{1}{1 + \frac{2\sqrt{2} \times 0.468 \times 24 \times 11.5 \times 10^3}{0.584 \times 11.53 \times 30 \times 10^3}}$$

Giving: $= 0.458$

Therefore:

$$\theta_y = \frac{7{,}580}{24} \frac{(108-24)}{(108-12)} \left\{ 0.453 \times 10^{-5} + \frac{(1 + 0.458)}{12 \times 0.775 \times 30 \times 10^3} \right\}$$

Giving:

$$\theta_y = 0.00269 \text{ radians}$$

7) Delfection Between End Pins at the Yield Load

From Eq (18)

$$\delta_y = 2 \frac{M_r \; a^2}{3EI} + \frac{\theta L}{2}$$

Hence:

$$\delta_y = 2 \frac{7{,}580 \times 96^2}{3 \times 30 \times 10^3 \times 2987.3} + \frac{0.00269 \times 108}{2}$$

Giving:

$$\delta_y = 0.584 \text{ inches}$$

B. ELASTIC DESIGN OF WELDS

These welds are proportioned to follow Section 15 of the A.I.S.C. Specification at a load at which tha maximum combined stress in the rolled section at the edge of the connection is 20 ksi. At this point, the load on the connection would be 67.5 K (Eq 4) and the bending moment at the rolled section would be 4590 in-k. (Eq 5)

1) Fillet Weld For a Possible Lap Joint of End Plate to Flange of Column

Since the flange force must be transferred to the end plate, the area of weld required is

$$A = \frac{\text{Flange Force}}{13.6} = \frac{\text{Allowable Plastic Stress x Plate area}}{\text{Allowable Weld Stress}}$$

$$= \frac{20 \times 12 \times 0.775}{13.6}$$

$$= 13.68 \text{ in}^2$$

Hence the total length of weld required is

$$L = \frac{\text{Area Weld}}{0.707\ D}$$

Giving:

D = 3/8 in; L = 51.6 in.

D = 1/2 in; L = 38.7 in.

It is evident that too great a length of lap joint is required using fillet welds. Therefore as a matter of economy a butt weld would be more suitable to use.

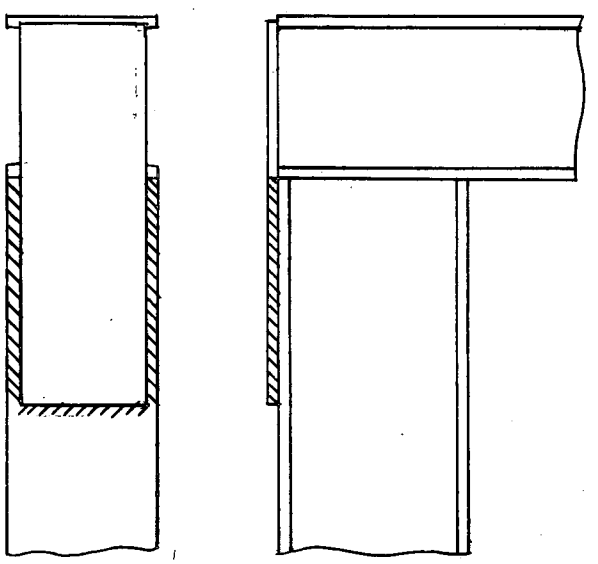

Fig A.3

2) Fillet Welds between Column Web and Beam Flange

The tensile or compressive direct stress on the weld is

$$\sigma_D = P/A\sqrt{2}$$

$$\sigma_D = \frac{67.5}{\sqrt{2} \times 24.98}$$

$$= 1.622 \text{ k/in}^2$$

The direct force per inch of weld is then:

$$f_D = \sigma_D \frac{w}{2}$$

$$= \frac{1.622 \times 0.468}{2}$$

$$= 0.33 \text{ k/in}$$

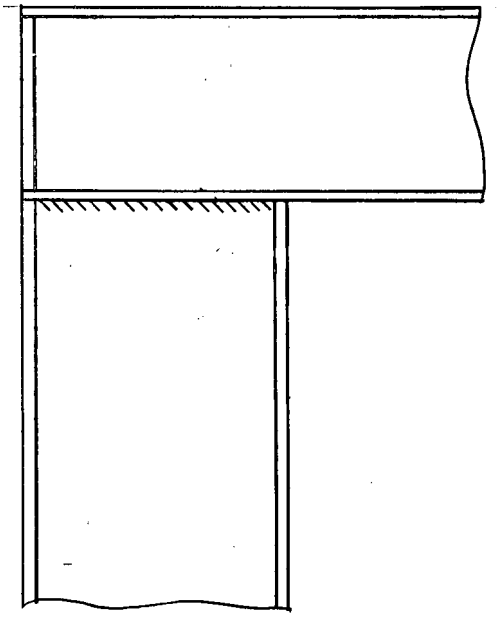

Fig A.4

The maximum force per inch due to bending in the web

$$f_m = \frac{3M_w}{L^2}$$

where

$$M_w = M - M_f$$

and

$$M_f = F(d-t)$$

$$M_w = 4.590 - 186\ (24-0.775)$$

Giving: $M_w = 280$ in-k

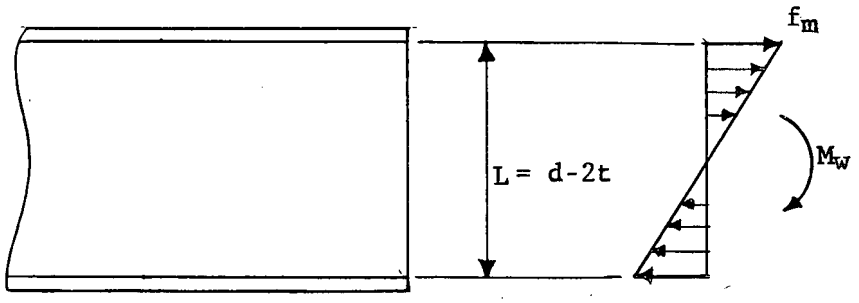

Fig A.5

Hence:

$$f_m = \frac{3M_w}{L^2}$$

$$= \frac{3 \times 280}{22.45^2}$$

$$= 1.664 \text{ k/in}$$

The force per inch per line of welding due to shear

$$f_v = \frac{P}{2}\sqrt{2}\ (d-2t)$$

Hence:

$$f_v = \frac{67.5}{2\sqrt{2} \times 22.45}$$

Giving:

$$= 1.062 \text{ k/in}$$

Therefore resultant vector

$$R = \sqrt{(f_D + f_m)^2 + f_v^2}$$

$$R = \sqrt{(1.664 + 0.38)^2 + 1.062^2}$$

$$= 2.30 \text{ k/in}$$

Hence the size fillet weld required is

$$D = \frac{R}{0.707 \times 13.6}$$

$$= \frac{2.30}{0.707 \times 13.6}$$

$$= 0.24 \text{ inches}$$

Nominal Size = 1/4 in.

3) Forty-Five Degree Fillet Welds at Ends of Diagonal Stiffener

The force in the diagonal stiffener is given by Eq 26

$$F_s = \sqrt{2}\, K_2 \times \text{Flange Force}$$

Hence:

$$F_s = \sqrt{2} \times 0.458 \times 20 \times 12 \times 0.775$$

$$= 106.6 \text{ kips}$$

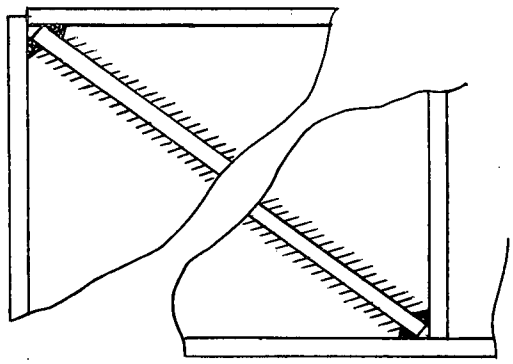

Fig A.6

The force per inch of weld

$$= \frac{P_s}{2b - w}$$

$$= \frac{106.6}{24-0.468}$$

Giving:

$$= 4.61 \text{ k/in}$$

Therefore the size fillet weld required is

$$D = \frac{\text{Force per inch}}{12.6 \cos 22.5^\circ}$$

$$= \frac{4.61}{13.6 \times 0.9239}$$

Giving:

$$= 0.367 \text{ inches}$$

Nominal Size = 3/8 in.

4) Fillet Weld for Web of Beam to End Plate

In sections 4 and 5 the expressions for the required fillet welds are not derived. To determine how these are obtained one can refer to section 17 (Design of Welds).

Size of fillet weld required

$$D = \frac{\text{Flange Force}}{2(d-2t)\ 13.6 \times 0.707}$$

Hence

$$D = \frac{20 \times 12 \times 0.775}{2 \times 22.45 \times 13.6 \times 0.707}$$

Giving:

$$= 0.431 \text{ inches}$$

Nominal Size = 7/16 in.

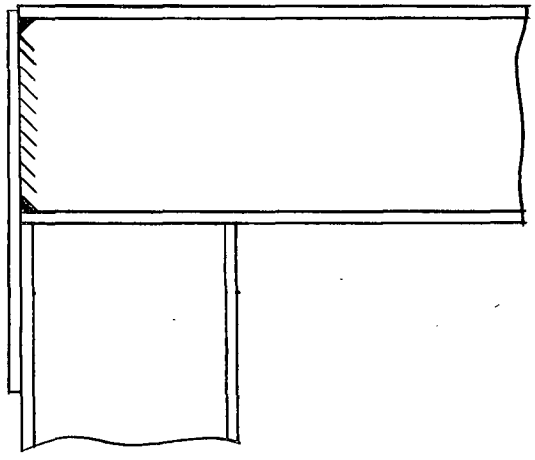

Fig A.7

5) Fillet Weld Required between Column Flange and Beam Flange

Size fillet weld required

$$D = \frac{\text{Flange force}}{(2b-w)\ 13.6 \times 0.707}$$

$$= \frac{20 \times 12 \times 0.775}{(24-0.468)\ 13.6 \times 0.707}$$

Giving: 0.823 inches

Nominal Size: = 7/8 in.

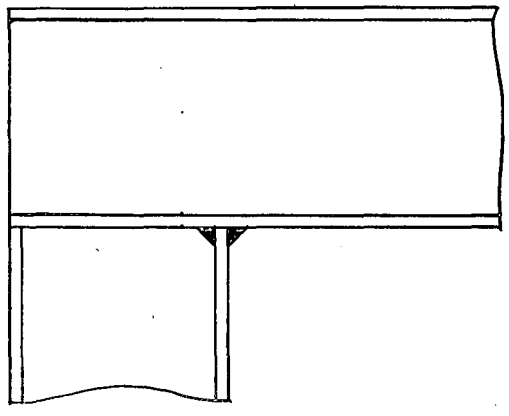

Fig A.8

Hence a butt weld would be more satisfactory at this point.

6) Fillet Welds Between Vertical Half Depth Stiffener and Web of Beam

The allowable compressive force to be carried by the web is from Eq 26

$$P_W = 24w\ (t + 2k)$$

$$= 24(0.468)\ (0.775 \times 3.125)$$

$$= 43.8 \text{ kips}$$

Hence the force to be carried by the vertical stiffener is

$$F_s = P_F - P_w$$

where P_F is the flange force

P_F = allowable plate stress x plate area

$P_F = 20\ (12)\ (0.775)$

$= 186$ kips

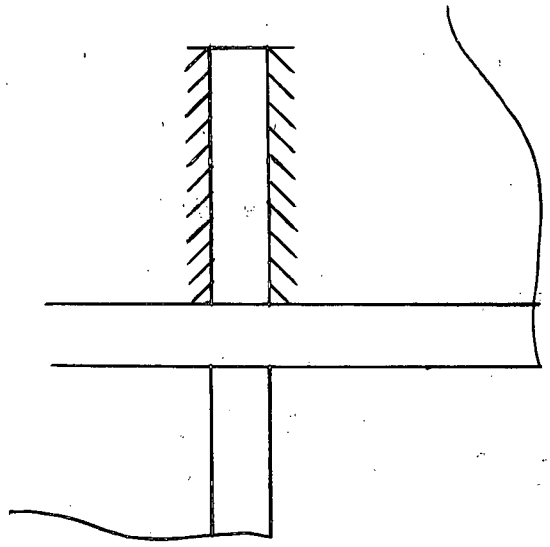

Fig A.9

Therefore:

$$F_s = 186 - 43.8$$

$$= 142.2 \text{ kips}$$

Therefore the size fillet weld required is

$$D = \frac{F_s}{4 \times 0.707 \times 13.6\ (d/2 - k)}$$

$$= \frac{142.2}{4 \times 0.707 \times 13.6\ (12 - 1.56)}$$

$$= 0.332 \text{ inches}$$

Nominal Size = 3/8 in.

C. PLASTIC ANALYSIS OF WELDS

In this section, the sizes of welds to meet the requirements of section 12 of this report at the maximum load of the connection are calculated.

1) Possible Fillet Weld for Lap Joint of End Plate to Flange of Column (Fig A.3)

Area of weld required Eq (25)

$$A = \frac{\text{Flange Force}}{22.4}$$

$$= \frac{307}{22.4}$$

Gives: $= 13.7 \text{ in}^2$

Hence the length of the weld required Eq (24):

$$L = \frac{\text{Area}}{0.707D}$$

Therefore:

$$D = 5/16 \text{ in}; \qquad L = 62.0 \text{ in}$$

$$D = 7/16 \text{ in}; \qquad L = 44.3 \text{ in}$$

A butt weld is found to be more suitable in this case.

2) Column Web Fillet Weld to Beam Flange (Fig A.4)

Direct tensile or compression force per inch of weld

$$f_D = 33\ w/2$$

$$= 33 \times \frac{0.468}{2}$$

Gives: $= 7.72$ k/in

Force per inch due to shear

$$f_V = \frac{\sqrt{2}\ Pu}{4(d-2t)}$$

$$= \frac{133}{2\sqrt{2} \times 22.45}$$

Gives: $= 2.1$ k/in

Therefore resultant force per inch

$$R = \sqrt{f_D^2 + f_V^2}$$

$$R = \sqrt{2.1^2 + 7.72^2}$$

Gives: $= 8.0$ k/in

Hence Eq 21:

$$D = \frac{R}{0.707 \times 22.4}$$

$$= \frac{8.0}{0.808 \times 22.4}$$

Gives: $= 0.508$ inches

Nominal Size= 9/16 in.

3) Forty-Five Degree Fillet Welds to Ends of Diagonal Stiffener (Fig A.6)

Force in the diagonal stiffener, Eq (26)

$$F_s = \sqrt{2} K_2\ \sigma_y\ bt$$

$$= \sqrt{2} \times 0.458 \times 33 \times 12 \times 0.775$$

Gives: $= 176.4$ kips

Hence from Eq (27)

$$D = \frac{F_s}{22.4 \times 2\ (b-w) \cos 22.5^{o}}$$

$$= \frac{176.4}{22.4 \times 2\ (12-0.468)\ 0.9239}$$

Gives: $= 0.370$ inches

Nominal Size $= 3/8$ inches

4) End Plate to Beam Web (Fig A.7)

Plastic flange force

$$P_F = \sigma_y\ bt$$

$$= 33 \times 12 \times 0.775$$

Gives: $P_F = 307$ kips

Therefore size fillet weld required Eq (23)

$$D = \frac{P_F}{0.707 \times 22.4 \times 2\ (d-2t)}$$

$$= \frac{307}{0.707 \times 22.4 \times 2 \times 22.45}$$

Gives: $= 0.434$ inches

Nominal Size $= 7/16$ inches

5) Possible Fillet Welds to Connect Column Flange to Beam Flange (Fig A.8)

Required size of fillet weld Eq (20)

$$D = \frac{\text{Flange force}}{0.707 \times 22.4\ (2b-w)}$$

$$= \frac{307}{0.707 \times 22.4 \times 23.53}$$

Gives: $= 0.829$ inches

Nominal Size $= 7/8$ inches

Hence a butt weld is found to be more suitable in this case.

6) Fillet Welds between Vertical Half Depth Stiffener and Web of Beam (Fig A.9)

Flange force to be carried by the web is Eq (28)

$$P_W = \sigma_y\ w\ (t + 2k)$$

$$= 33 \times 0.468\ (0.775 + 3.125)$$

Gives: 60.2 kips

Hence the force in the vertical stiffener is

$$F_s = P_F - P_W$$

$$= 307 - 60.2$$

Gives: $= 246.8$ kips

Therefore size fillet weld from Eq (29)

$$D = \frac{F_s}{4 \times 0.707 \times 22.4\ (d/2 - k)}$$

Therefore: $$D = \frac{246.8}{4 \times 0.707 \times 22.4\ (12 - 1.56)}$$

Gives: $= 0.350$ inches

Nominal Size = 3/8 in.

12. APPENDIX B

ANALYSIS OF STRAIGHT KNEES WITH DIAGONAL STIFFENERS

Two analyses are considered in this appendix: (a) an analysis leading to a required thickness of diagonal stiffener to prevent undue deformation of the knee web due to shear force, and, (b) an analysis of the rotation of a straight knee with diagonal stiffeners.

(a) Diagonal Stiffeners for Straight Connections

From Ref 1 and referring to Fig B.1

$$F_o = \frac{M_h}{d}(1 - d/L) \qquad \ldots (1)$$

where M_h = moment at point H

d = depth of section

L = length of connections leg

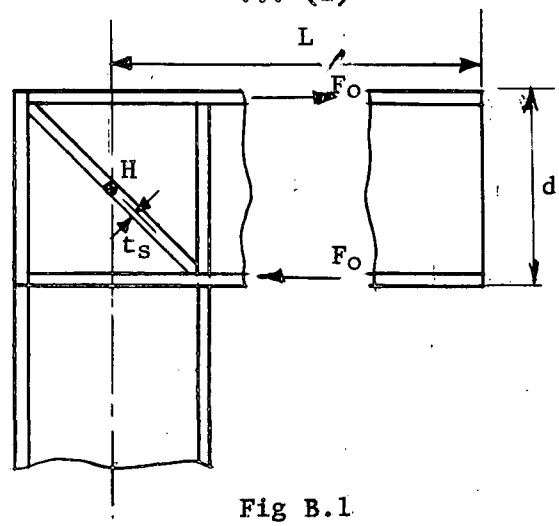

Fig B.1

The desired moment at point H is Mp. Therefore Eq (1) becomes

$$F_o = \frac{\sigma_y Z}{d}(1 - d/L) \qquad \ldots (2)$$

The force F_o is resisted by the web acting in shear and the diagonal stiffener acting in compression. The shear resistance of the web, F_w, is given by

$$F_w = \frac{\sigma_y}{\sqrt{3}} wd \qquad \ldots (3)$$

(where w = the thickness of the web) and the resistance of the diagonal stiffener is given by

$$F_s = \sigma_y \frac{bt_s}{\sqrt{2}} \qquad \ldots (4)$$

Since $F_o = F_w + F_s$, then from Eqs (2), and (3) and (4)

$$\frac{\sigma_y Z}{d}(1 - d/L) = \frac{\sigma_y}{\sqrt{3}} wd + \frac{\sigma_y}{\sqrt{2}} bts \qquad \ldots (5)$$

Solving this equation for t_s,

$$t_s = \frac{\sqrt{2}}{b}\left(\frac{Z\,(1-d/L)}{d} \quad \frac{wd}{\sqrt{3}}\right) \qquad \ldots (6)$$

Since $Z = fS$, and since the quantity $f\,(1 - d/L)$ is very nearly equal to 1.0, Eq (6) reduces, finally to

$$t_s = \frac{\sqrt{2}}{b}\left(\frac{S}{d} - \frac{wd}{\sqrt{3}}\right) \qquad \ldots (7)$$

which gives the required thickness of diagonal stiffener in order that the connection be capable of resisting the plastic moment, M_p, applied at the intersection of neutral lines of the beam and girder.

(b) <u>Rotation Analysis of Straight Knees with Diagonal Stiffeners</u>*

The rotation of the knee is made up of two parts:

1) Rotation due to shear, designated as γ, and
2) Rotation due to bending, designated as β.

Since comparisons are made with experimentally determined rotation values there is a third component to be considered if the measurement is made at a point other than at the precise end of the connection:

3) Rotation due to bending of the rolled section over the length, r, between the end of the knee and point of rotation measurement, designated as ϕ_r.

Hence the total knee rotation is $\theta = \gamma + \beta + \phi_r$ ... (8)

---

* Based in part on Ref 7, Appendix A.

Two different appraoches were used in Ref 1 to predict the moment-rotation characteristics of straight knees with diagonal stiffeners. It is the purpose of this section to refine the solution of this problem.

Rotations due to shear in the square knee A B C D (Fig B.2) reinforced with diagonal stiffeners will be found by making the same assumption that was implied in section (a) above: the flange force F_o is resisted in part by the knee web and in part by the component of thrust from the diagonal stiffener AC.

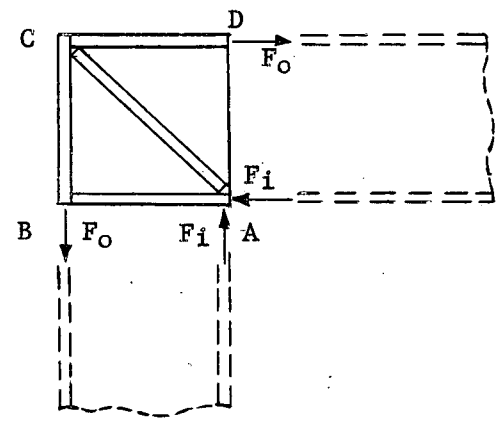

Fig B.2

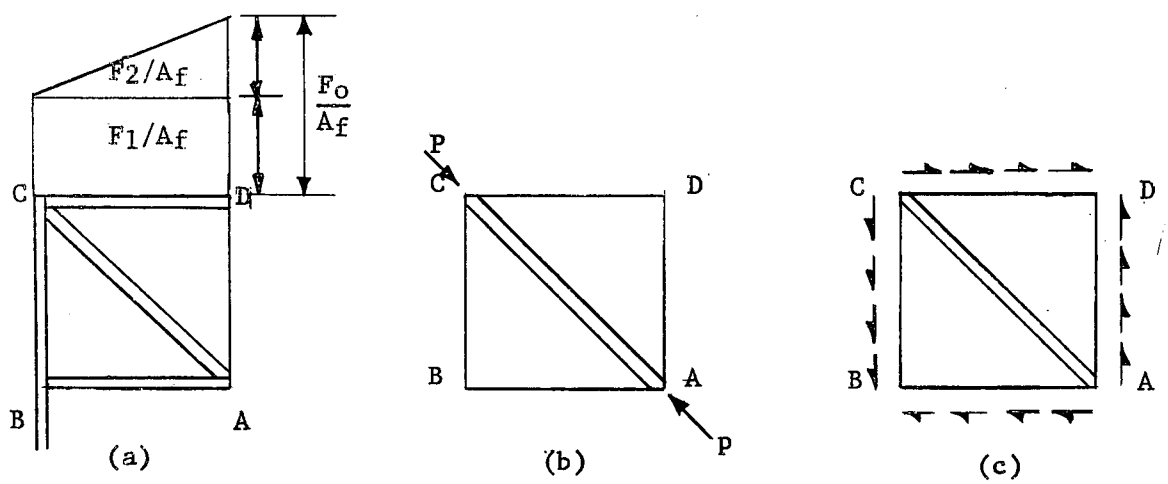

(a) (b) (c)

Fig B.3

Thus in Fig B.3-a although the decrease in stress is linear from D to C, the flange at point C retains a stress of magnitude F_1/A_F. The resultant force is transmitted to the diagonal stiffener.

The problem to be solved, then, is the relation between the force F_2 transmitted by the exterior flange to the web due to shearing action (represented by the triangular distribution in Fig B.2-a) and the force F_1 transmitted to the diagonal stiffener. This may be done by connecting the continuity condition at point C; then the moment-shear deformation relationship may be developed.

Consider the plate A B C D with diagonal stiffener and loaded with end compressive forces, P, as shown in Fig B.3-b. This simulates the loading applied to the stiffener by the flange force F_1. Fig B.3-c shows the shear stresses acting on the web, the stresses introduced by the flange force F_2. The variation in normal stress along the stiffener due to the loading of Fig B3.b would resemble Fig B.4-a; the stress will decrease

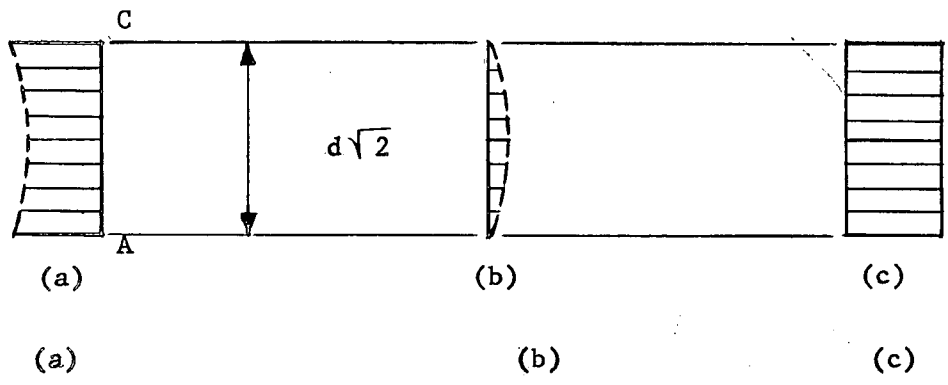

Fig B.4

toward the center of the plate as the stiffener transmits load to the plate by shear. On the other hand, the shear loading of Fig B.3-c will cause stresses along the stiffener somewhat like those of Fig B.4-b. Normal stresses will gradually increase towards the center of the stiffener.

When the two loadings of Fig B.3-b and -c are added together to give the loading due to the flange force, F_o, it will be assumed that the resultant stresses in the stiffener are uniform as shown in Fig B.4-c. It will be assumed that the web plate remains in a state of pure shear and the contraction along line AC of Fig B.3-c will thus remain uniform.

Since the total shortening of the stiffener must equal the contraction due to the shear stresses in order that the continuity condition be satisfied, then in the general case (referring to Fig B.5)

$$\int_o^a \epsilon_{w(x)} \, d_x = \int_o^a \epsilon_{s(x)} \, d_x \qquad \ldots (9)$$

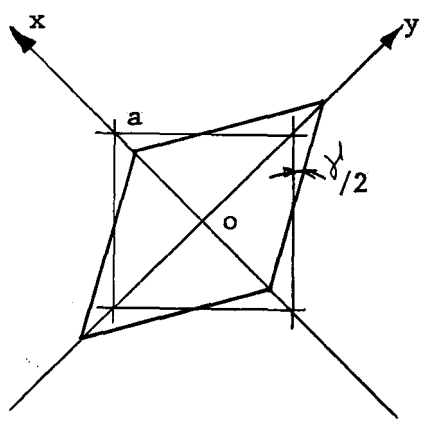

Fig B.5

where the subscripts w and s refer to web and stiffener, respectively. According to the assumptions made above, Eq (9) reduces in this problem to[8]

$$\gamma/2 = \epsilon_x \qquad \ldots (10)$$

where the subscripts w and s have been dropped, being uniform and equal along line AC. Now

$$\gamma = \frac{\tau}{G}; \epsilon_x = \frac{x}{E} \qquad \ldots (11)$$

and

$$\tau = \frac{F_2}{A_w}; \sigma_x = \frac{P}{A_s} = \frac{F_1\sqrt{2}}{A_s} \qquad \ldots (12)$$

Therefore, from Eq (10)

$$\frac{F_2}{2A_WG} = \frac{F_1\sqrt{2}}{A_s\ E}$$

or

$$F_2 = \frac{2Aw\ \ G\sqrt{2}}{A_s\ E}\ F_1 \qquad \ldots (13)$$

But

$$F_1 + F_2 = F_o \qquad \ldots (14)$$

and therefore, if we let

$$K_1 = 2A_wG\sqrt{2}/A_sE \qquad \ldots (15)$$

then

$$F_1 + K_1\ F_1 = F_o$$

or

$$F_1 = \frac{F_o}{1+K_1} = K_2\ F_o \qquad \ldots (16)$$

where

$$K_2 = \frac{1}{1 + \frac{2A_wG\sqrt{2}}{A_s\ E}} \qquad \ldots (17)$$

Similarly,

$$F_2 = (1-K_2)\ F_o \qquad \ldots (18)$$

The rotation of the knee due to these forces is equal to γ. Since (Ref 1)

$$F_o = \frac{M_h}{L}\ (\frac{L}{d} - 1) \qquad \ldots (19)$$

Then equations (18) and (19) and the first of Equations (11) and (12) may be used to determine the moment-deformation (shear) relationship. Making the substitutions,

$$\gamma = K_3\ \frac{M_h}{d}\ (1 - d/L) \qquad \ldots (20)$$

where

$$K_3 = \frac{1-K_2}{G\ A_w} = \frac{1}{Gwd + \frac{t_s\ b_s\ E}{2\ \sqrt{2}}} \qquad \ldots (21)$$

According to assumptions made above, the extension of the flanges, δ, will be given by

$$\delta = \left(\frac{\sigma_D + \sigma_C}{2}\right) \frac{d}{E} \qquad \ldots (22)$$

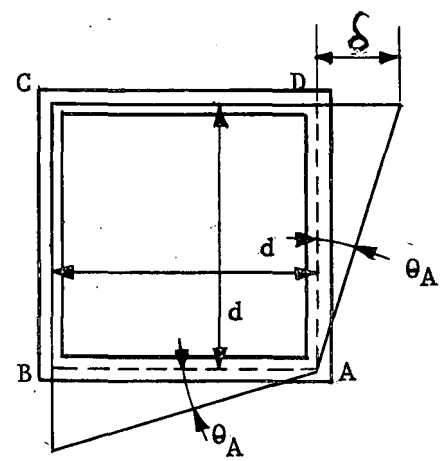

Fig B.6

Using Fig B.6, the total "bending" rotation at the knee is

$$\beta = 2\ \theta_a = 2\ \frac{\delta}{d} = \frac{\sigma_D + \sigma_C}{E}$$

Now from Fig B.3-a and Eq (16)

$$\sigma_C = \frac{F_1}{F_o}\ \sigma_D = K_2\ \sigma_D$$

and from Fig B.3-a and Eq (19)

$$\sigma_D = \frac{M_h}{LA_F}\ \left(\frac{L}{d} - 1\right)$$

Then the total bending rotation is given by

$$\beta = (1+K_2)\ \frac{M_h}{A_f\ dE}\ (1 - d/L) \qquad \ldots (23)$$

The rotation, ϕ_r, due to flexure of the rolled section over lengths r is given by

$$\theta_r = \frac{M_r}{EI}(2r - r^2/a) \qquad \ldots (24)$$

therefore

$$\theta_r = \frac{M_h}{EI}(1 - d/2L)(2r - r^2/a) \qquad \ldots (25)$$

When r is small the term r^2/a may be neglected. Then the total rotation is given by a summation of the values determined from (20) (23), and (25)

or

$$\theta = \gamma + \beta + \theta_r \qquad \ldots (8)$$

$$\theta = K_3 \frac{M_h}{d}(1-d/L) + (1+K_2)\frac{M_h}{A_F dE}(1 - d/L) + \frac{M_h}{EI}(1 - d/2L)(2r - r^2/a) \qquad \ldots (26)$$

$$\theta = M_r \frac{(1-d/L)}{(1-d/2L)}\left\{\frac{K_3}{d} + \frac{(1+K_2)}{A_F dE} + \frac{(1 - d/2L)}{(1-d/L)}\frac{(2r - r^2/a)}{EI}\right\} \qquad \ldots (27)$$

The results of this analysis of shear and bending deformations are compared with experimental results for two tests using WF shapes of widely differing geometry in Fig B.7. The initial portion of the moment rotation curve of Connection L[1] is shown in Fig B.7-a, Eq (27) being used to plot the theoretical curve shown by the dotted line. In Fig B.7-b is a similar comparison using the results of a frame tests with an 8WF 40 shape. In the second case, load is plotted against the total rotation of the knee.

In view of the agreement between theory and test of two markedly different cross-sections, this anslysis affords a satisfactory explanation of experimental behavior.

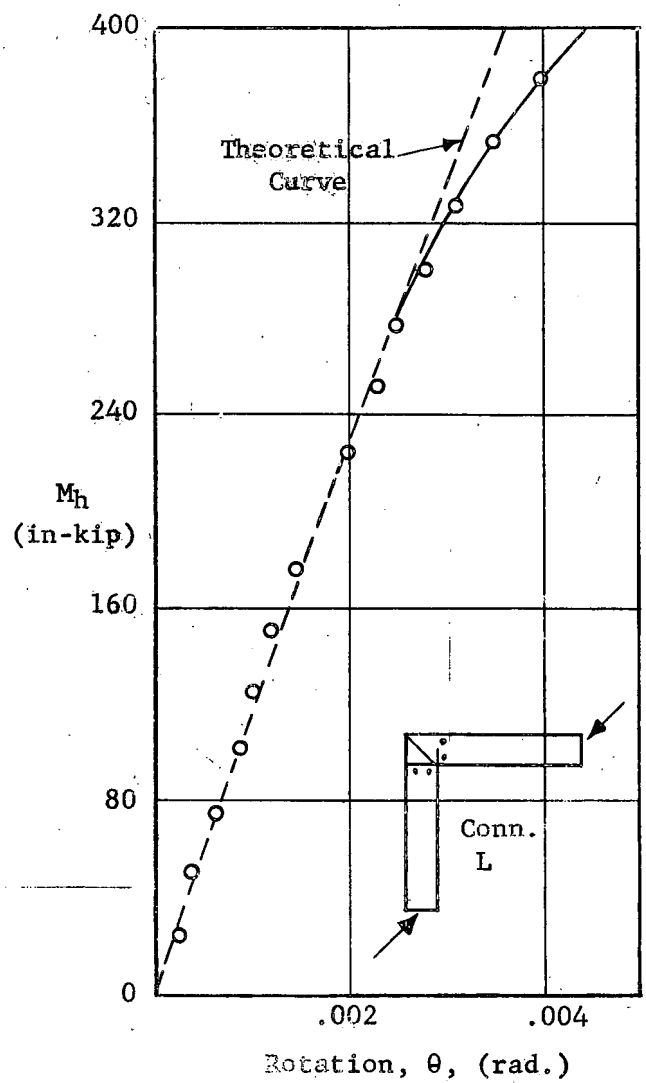

(a)- Moment-angle change relationship of Connection L at the knee. 8B13 shape.

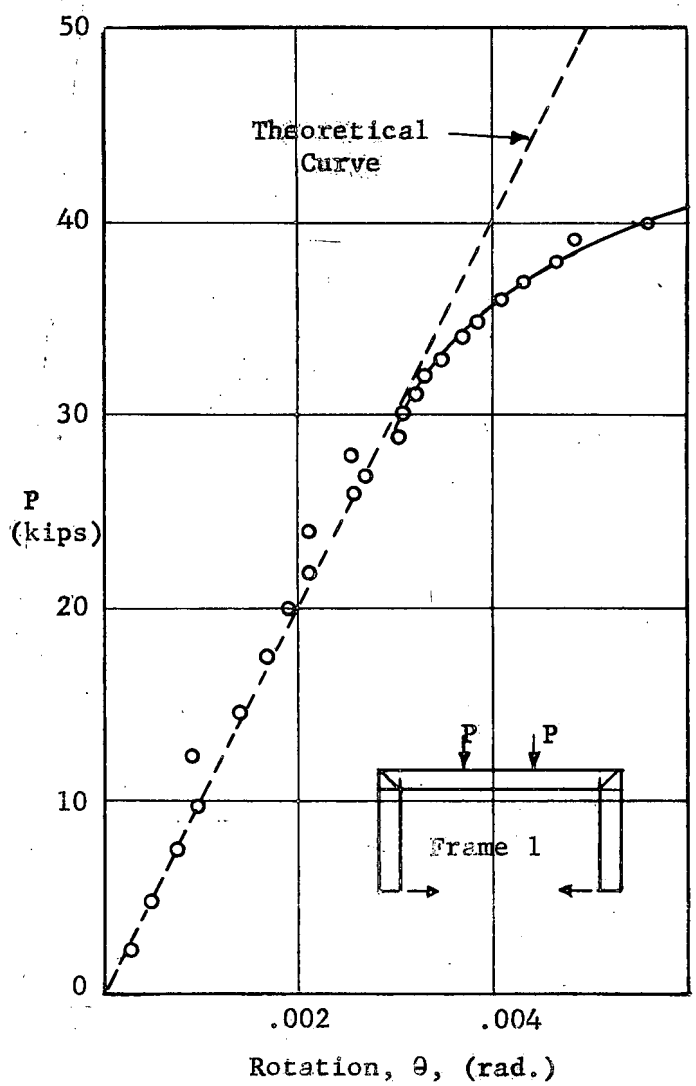

(b)- Rotation at knee with increase of load for Portal Frame 1. 8WF40 rolled shape.

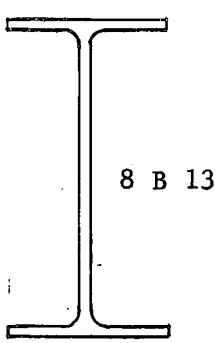

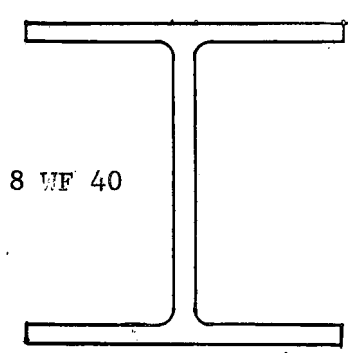

Fig B.7

TABLE 1
SUMMARY OF COUPON TEST RESULTS

Material				Average Coupon Test Results						
Test No.	Shape	Type Coupon	Location	σ_{yu} (ksi)	σ_{yL} (ksi)	σ_{ult} (ksi)	ε_y (in/in)	ε_{st} (in/in)	E (ksi)	E_{st} (ksi)
T-11	8B13	Tension	Flange	---	41.8	---	---	---	--	---
			Web	---	47.1	---	---	---	--	---
T-101	14WF30	Tension	Flange (3)*	36.9	36.3	61.2	0.00116	0.0173	--	736
			Web (1)	42.5	41.7	65.5	.00141	.0182	--	607
		Compres-	Flange (3)	39.0	38.5	--	.00129	.0119	30 050	757
		sion	Web (1)	44.5	44.5	--	.00149	.0100	30 050	761
		Avg.T &C	Flange (6)	38.0	37.4	--	.00122	.0146	--	746
			Web (2)	43.5	43.1	--	.00145	.0141	--	684
			Avg.-2+(8)	40.2	39.7	--	.00131	.0144	--	723
		Mill Rpt.°	Web (1)	43.61	--	70.55	--	---	--	---
T-102	24WF100	Tension	Flange (6)	36.0	34.9	62.4	.00121	.0135	--	646
			Web (4)	42.2	39.1	64.6	.00139	.0198	--	595
		Compres-	Flange (6)	36.1	35.2	--	.00122	.0104	29 400	844
		sion	Web (3)	41.5	40.5	--	.00139	.0154	29 800	642
		Avg.T& C	Flange (12)	36.0	35.0	--	.00122	.0120	--	790
			Web (7)	41.9	39.7	--	.00139	.0179	--	615
			Avg.-2+(19)	38.2	36.7	--	.00128	.0142	--	721
		Mill Rpt.°	Web (1)	41.11	--	64.01	--	---	--	---=
T-4 (205.5)	30WF108	Tension	Flange	36.9	34.8	60.6	.00137	---	--	---
			Web	39.1	38.1	62.2	.00175	.0205	--	577
T-103	36WF230	Tension	Flange (6)	36.1	35.6	64.2	.00125	.0128	--	660
			Web (4)	43.2	42.1	66.8	.00135	.0188	--	555
		Compres-	Flange (6)	37.1	36.2	--	.00127	.0100	29 100	903
		sion	Web (3)	44.0	43.0	--	.00149	.0164	29 500	756
		Avg.T&C	Flange (12)	36.6	35.9	--	.00126	.0114	--	782
			Web (7)	43.6	42.5	--	.00141	.0178	--	641
			Avg.-2+(19)	39.3	38.5	--	.00132	.0139	--	719
		Mill Rpt.°	Web (1)	47.62	--	69.47	--	---	--	---

* Number of Specimens
\+ Avg.-2 Weighted Average in Proportion to Flange and Web Areas
° Mill Report Tensile Test

TABLE 2

SECTION PROPERTIES OF TEST SPECIMENS

	Weight per Ft.	Area of Section	Depth of Section	Flange				Web Thickness	Axis x-x			
				Width	Average Thickness	Thickness at Toe	Thickness at Root		I	S	Z	f
		A	d	b	t	t'	t"	w				
	lb.	in^2	in.	in.	in.	in.	in.	in.	in^4	in^3	in^3	
8B13 (T-11)												
Handbook	13	3.83	8.00	4.00	0.254			0.230	39.5	9.88	(11.35)	(1.149)
Measured		3.99	8.06	4.03	0.266			0.237	42.1	10.42	12.01	1.152
%Variation		+4.18	+0.75	+0.75	+4.72			+3.04	+6.59	+5.47	+5.81	+0.26
14WF30 (T-101)												
Handbook	30	8.81	13.86	6.733	0.383	5/16	7/16	0.270	289.6	41.8	(47.1)	(1.127)
Measured	29.3	8.62	13.74	6.74	0.364	0.295	0.429	0.268	273.1	39.8	44.9	1.128
%Variation	-2.33	-2.16	-0.87	+0.10	-4.96	-5.60	-1.94	-0.74	-5.70	-4.78	-4.67	+0.09
24WF100 (T-102)												
Handbook	100	29.43	24.00	12.00	0.775	5/8	15/16	0.468	2 987.3	248.9	(278.3)	(1.118)
Measured	99.35	29.03	24.00	12.00	0.748	0.612	0.882	0.481	2 899.5	241.6	271.1	1.122
%Variation	-0.65	-1.36	0.00	0.00	-3.49	-2.18	-5.93	+2.78	-2.93	-2.93	-2.59	+0.36
30WF108 (205.5-T-4)												
Handbook	108	31.77	29.82	10.484	0.760	0.625	0.875	0.548	4 461.0	299.2	345.5	1.155
Measured		30.46	29.93	10.460	0.740	0.650	0.842	0.518	4 345.8	290.3	334.1	1.151
%Variation		-4.19	+0.37	-0.23	-2.63	+4.00	-3.93	-5.48	-2.59	-2.98	-3.31	-0.35
36WF230 (T-103)												
Handbook	230	67.73	35.88	16.475	1.260	1-1/16	1-7/16	0.765	14 988.4	835.5	(942.7)	(1.128)
Measured	228	67.15	35.91	16.34	1.24	1.055	1.42	0.786	14 748.1	821.2	929.1	1.131
%Variation	-0.87	-0.86	+0.08	-0.82	-1.59	-0.70	-1.22	+2.75	-1.60	-1.71	-1.44	+0.27

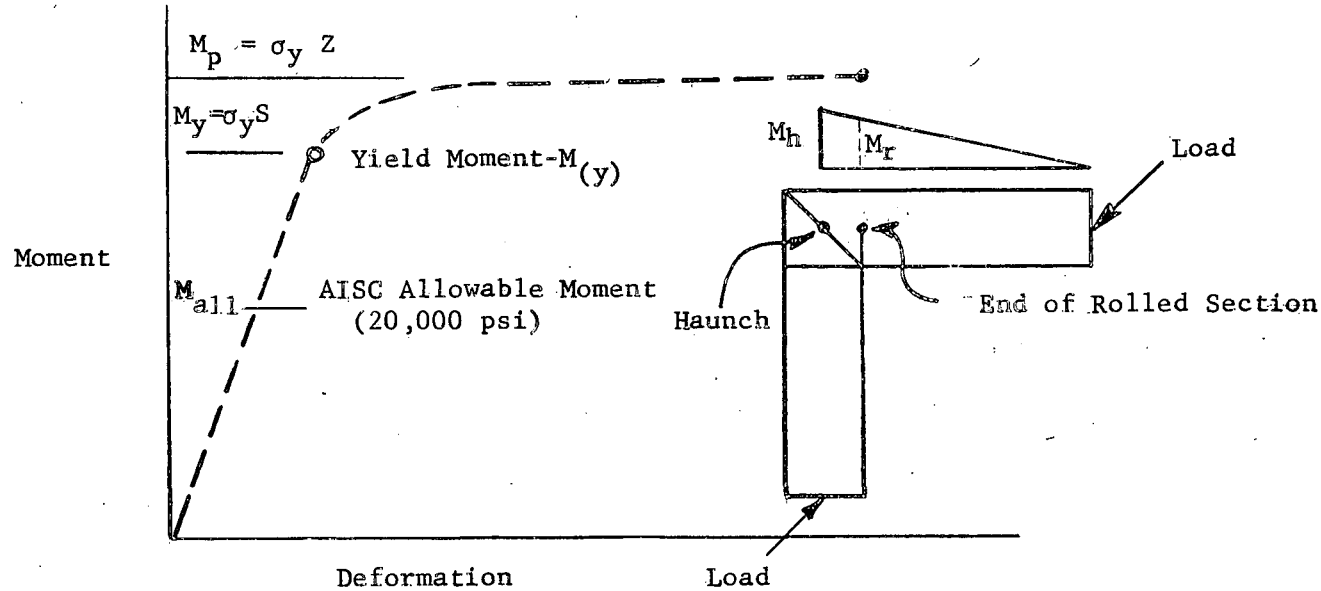

THEORETICAL MOMENTS

Section	Basis of Calculation **	Moments in Kip - Inches						
		Elastic Range				Plastic Range		
		M_y (parameter)	M allowable* (AISC)	$M_{h(y)}$*	$M_{r(y)}$*	M_p (parameter)	$M_{h(p)}$*	M_{pc}
8 B 13	Measured Handbook	435 326	193 183	454 340	403 302	502 374	559 417	496 369
14 WF 30	Measured Handbook	1488 1380	757 830	1530 1482	1412 1370	1734 1553	1870 1672	1725 1544
24WF100	Measured Handbook	8,450 8,210	4,440 4,590	8,750 8,500	7,775 7,580	9,750 9,170	10,820 10,160	9619 9027
36WF230	Measured Handbook	29,450 27,600	15,100 15,400	30,550 28,550	27,150 25,400	34,810 31,100	38,650 34,400	34,380 30,650
30WF108	Measured Handbook	10,100 9,870	5,360 5,540	10,500 10,260	9,345 9,140	11,601 11,400	12,930 12,700	11,500 11,300

Connection Test Nos. 4, 11, 101, 102 and 103

* M_{all}, M_h, & M_r were calculated considering the effect of axial load.

** "Measured" quantities calculated using measured dimensions and coupon stresses.

"Handbook" quantities calculated using AISC handbook dimensions and implied yield stresses. (33ksi)

TABLE 3

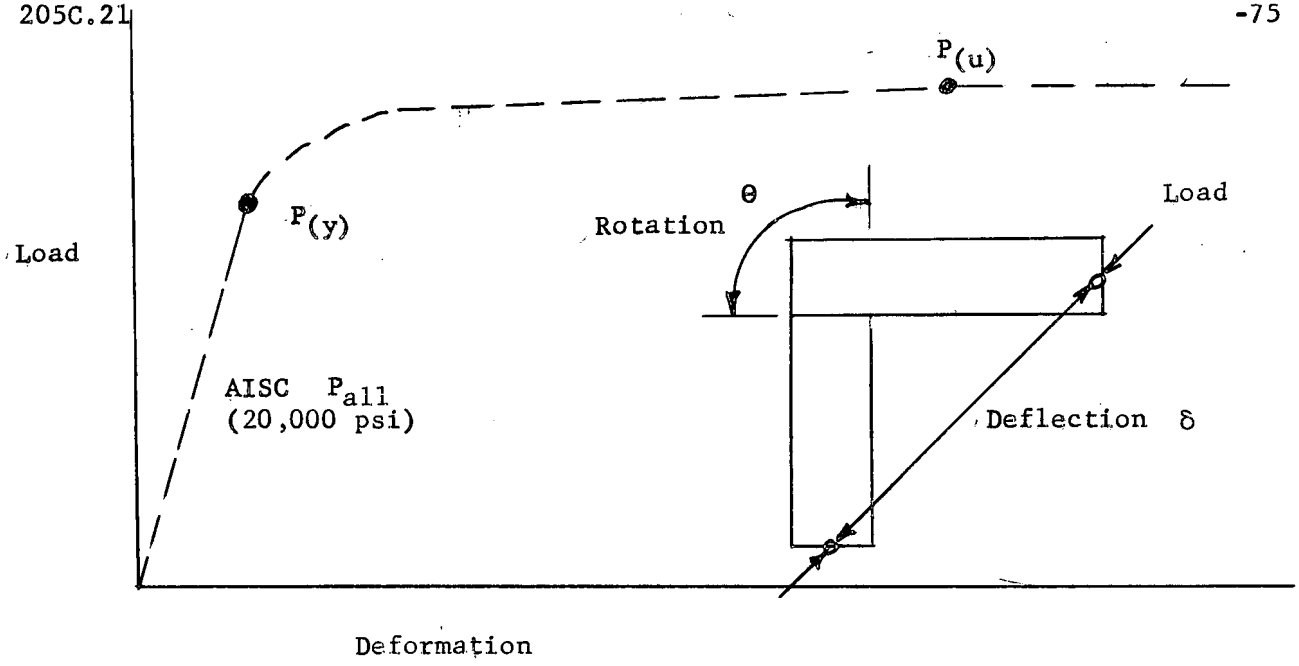

THEORETICAL LOADS AND DEFORMATIONS

Section	Basis for Calculation	Loads			Deformations		
		P_{all} (AISC)	$P_{(y)}$	$P_{(u)}$	$\delta_{(y)}$	$\theta_{(y)}$	ϕ_y (parameter)
		(kips)	(kips)	(kips)	(in)	(radians)	(rad/in)
8 B 13	Measured	8.69	18.12	25.2	0.230	0.00317	0.000350
	Handbook	8.23	13.58	16.64	0.186	0.00253	0.000285
14WF30	Measured	12.70	23.7	29.0	0.819	0.00378	0.000181
	Handbook	13.94	23.0	26.0	0.741	0.00303	0.000164
24WF100	Measured	65.5	114.3	141.5	0.626	0.00306	0.0000985
	Handbook	67.5	111.4	133.0	0.584	0.00269	0.0000946
36WF230	Measured	148.5	267	338	0.934	0.00280	0.0000681
	Handbook	151.0	249	301	0.856	0.00262	0.0000636
30WF108	Measured	63.2^k	110^k	135.5	0.738	0.00262	0.0000788
	Handbook	65.1	107.4	133.0	0.683	0.00249	0.0000789

Connection Test Nos. 4, 11, 101, 102 and 103

TABLE 4

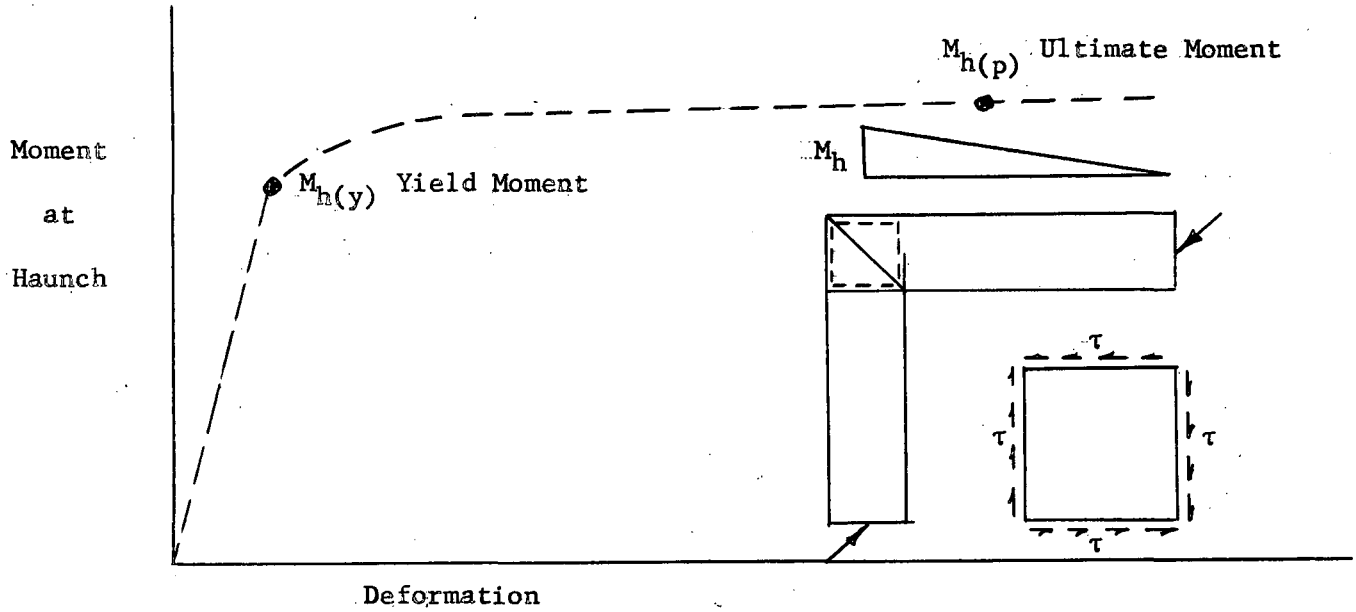

THEORETICAL SHEAR STRESSES
& WEB REINFORCEMENT

Section	Basis of Calculation	Shear Yield Strength of Web τ_y (ksi)	Shear Stress (ksi)				Reinforcement Required (in)	
			Without Diagonal Stiffener			With Diagonal Stiffener	Web Thickness Required w_r	Thickness of Diagonal Stiffener Required t_s
			τ at $M_h=M_{h(y)}$ *	τ at $M_h=M_{h(p)}$ *	τ at Elastic Web Buckling in Shear **	Used τ at $M_h=M_{h(p)}$		
8 B 13	Measured Handbook	27.2 19.05	22.8 17.84	28.0 21.9	217 203	19.82 14.93	0.280 0.270	0.074 0.069
14WF30	Measured Handbook	24.9 19.05	25.6 24.2	31.4 27.4	97.2 93.4	19.45 19.00	0.369 0.381	0.175 0.193
24WF100	Measured Handbook	23.0 19.05	24.6 24.4	30.4 29.2	101.0 93.5	18.10 17.15	0.734 0.756	0.428 0.487
36WF230	Measured Handbook	24.6 19.05	23.5 22.6	29.7 27.2	119.5 111.6	18.25 16.48	1.115 1.135	0.616 0.690
30WF108	Measured Handbook	22.0 19.05	17.65 16.40	21.75 20.3	75.5 84.0	15.15 14.84	0.569 0.588	0.125 0.098

* When τ exceed τ_y the stress is meaningless and indicates a stiffener is required.

** These are not true stresses and only indicate that web buckling due to shear is not a problem.

Connection Test Nos. 4, 11, 101, 102, and 103

TABLE 5

FILLET WELDS: COMPARISON OF PLASTIC AND ELASTIC DESIGN

	PLASTIC* DESIGN	ELASTIC DESIGN	ACTUALLY USED
Flange of Column to Flange of Beam			
8 B 13	5/16	5/16	3/16
14WF30	7/16	7/16	7/16
24WF100	7/8	7/8	Butt Weld
30WF108	7/8	13/16	Butt Weld
36WF230	1-3/8	1-3/8	Butt Weld
Web of Column to Flange of Beam			
8 B 13	1/4	3/16	3/16
14WF30	5/16	5/16	5/16
24WF100	9/16	1/4	9/16
30WF108	5/8	7/16	5/8
36WF230	7/8	7/16	7/8
Web of Beam to End Plate			
8 B 13	3/16	3/16	3/16
14WF30	1/4	1/4	5/16
24WF100	7/16	7/16	9/16
30WF108	5/16	5/16	5/16
36WF230	11/16	11/16	7/8
End Plate - Lap Joint to Flange of Column			
8 B 13	3/16 11.28"	3/16 11.3"	3/16 17"
14WF30	5/16 17.2"	5/16 17.1"	5/16 21"
24WF100	7/16 44.3"	7/16 44.2"	Butt Weld
30WF108	7/16 44.3"	7/16 44.3"	Butt Weld
36WF230	9/16 74.9"	9/16 76.6"	Butt Weld
Half Depth Vertical Stiffener to Beam Web			
8 B 13	1/8	1/8	3/16
14WF30	3/16	3/16	5/16
24WF100	3/8	3/8	5/16
30WF108	1/4	1/4	1/4
36WF230	1/2	1/2	3/8
Diagonal Stiffener to Flange End Plate and Vert. Stiff. 45° Fillet			
8 B 13	1/8	1/8	3/16
14WF30	3/16	3/16	5/16
24WF108	3/8	3/8	3/8
30WF108	1/4	1/4	1/4
36WF230	9/16	5/8	9/16

*Based on Handbook Properties and σ_y = 33,000 psi
Weld Stresses 33,000 psi tension and compression, 22,400 psi shear

Connection Test Nos. - 4, 11, 101, 102, and 103

TABLE 6

TABLE 7

CHEMICAL PROPERTIES

Description	Heat No.	C	M_n	P	S	Remarks
8 B 13	34Y532			.024	.030	A7-46
14WF30	41K525			.023	.044	A7
24WF100	44D508	0.18	0.56	.016	.039	A7-52T
30WF108	44G451	.20	.60	.01	.030	A7-53T
36WF230	35D654	.19	.70	.014	.032	A7-52T

Connection Test Nos. - 4, 11, 101, 102 and 103

TABLE 8

F/P_y (%) FOR LATERAL SUPPORT DYNAMOMETERS

		1	2	3	4
8 B 13	Point A	0.102	0.53	0.284	0.605
	Point B	0.114	1.21	0.865	0.651
14WF30	Point A	0.607	-0.0017	0.534	-0.058
	Point B	0.562	0.113	0.574	-0.038
24WF100	Point A	-0.0344	0.588	0.845	0.034
	Point B	-0.193	0.961	1.26	-0.0323
30WF108	Point A	0.1455	0.0940	.185	0.0158
	Point B	0.0485	0.109	0.0615	-0.0079
36WF230	Point A	0.0086	0.300	0.350	0.0288
	Point B	-0.560	0.915	1.433	0.067

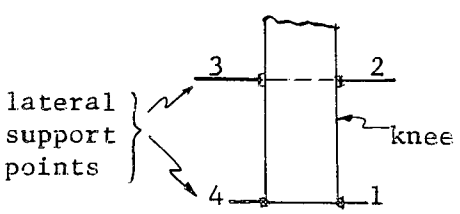

F = Force in dynamometers

$P_y = \sigma_y A = 33$ (A)

Point A: - Force in lateral support after mechanism has formed.

Point B: - Force in lateral supports at maximum moment.

Note: - See Figure 15 for location of points A and B.

Connection Test Nos. 4, 11, 101, 102 and 103.

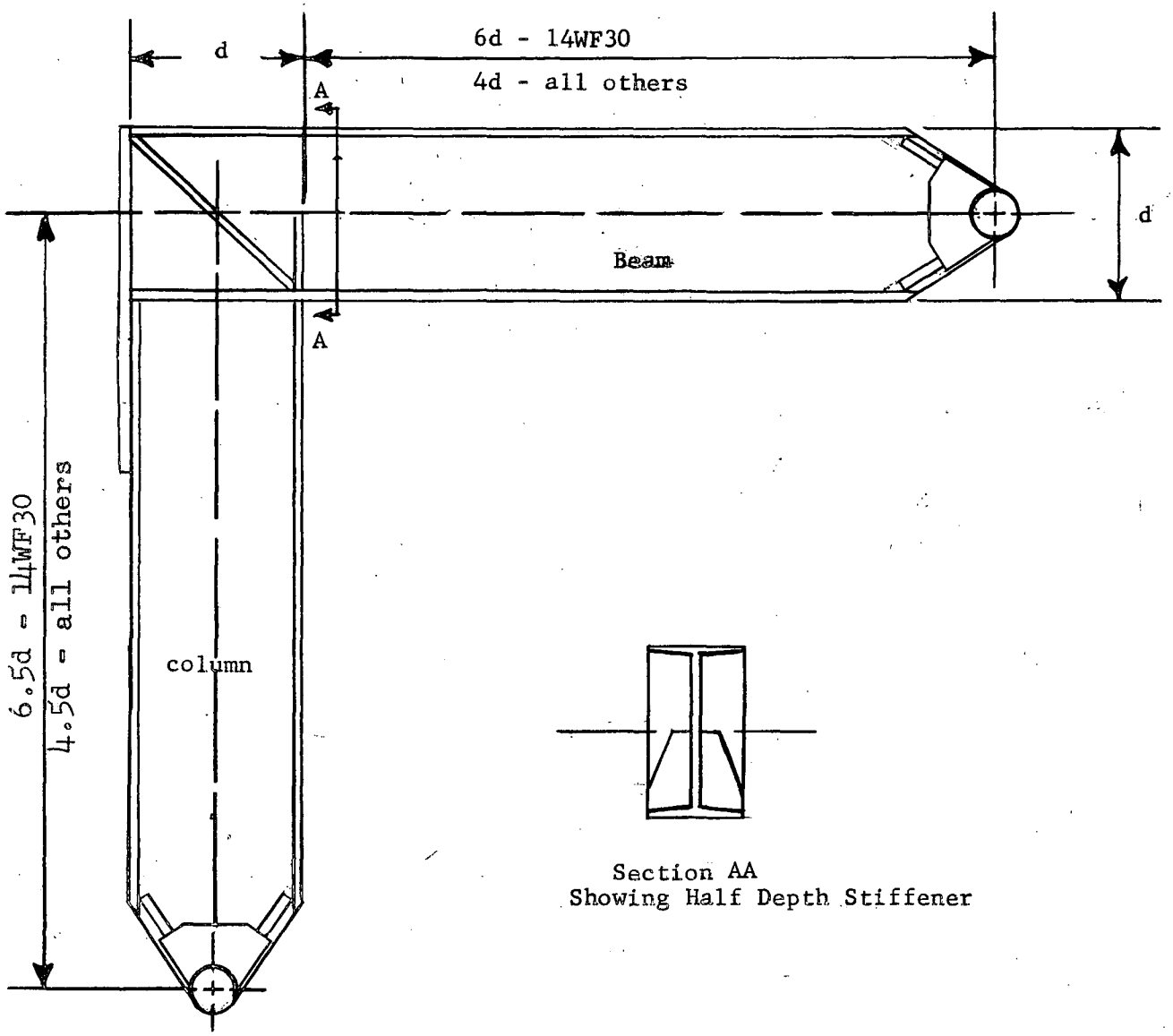

GENERAL VIEW SHOWING GEOMETRY OF CONNECTIONS

Figure 1

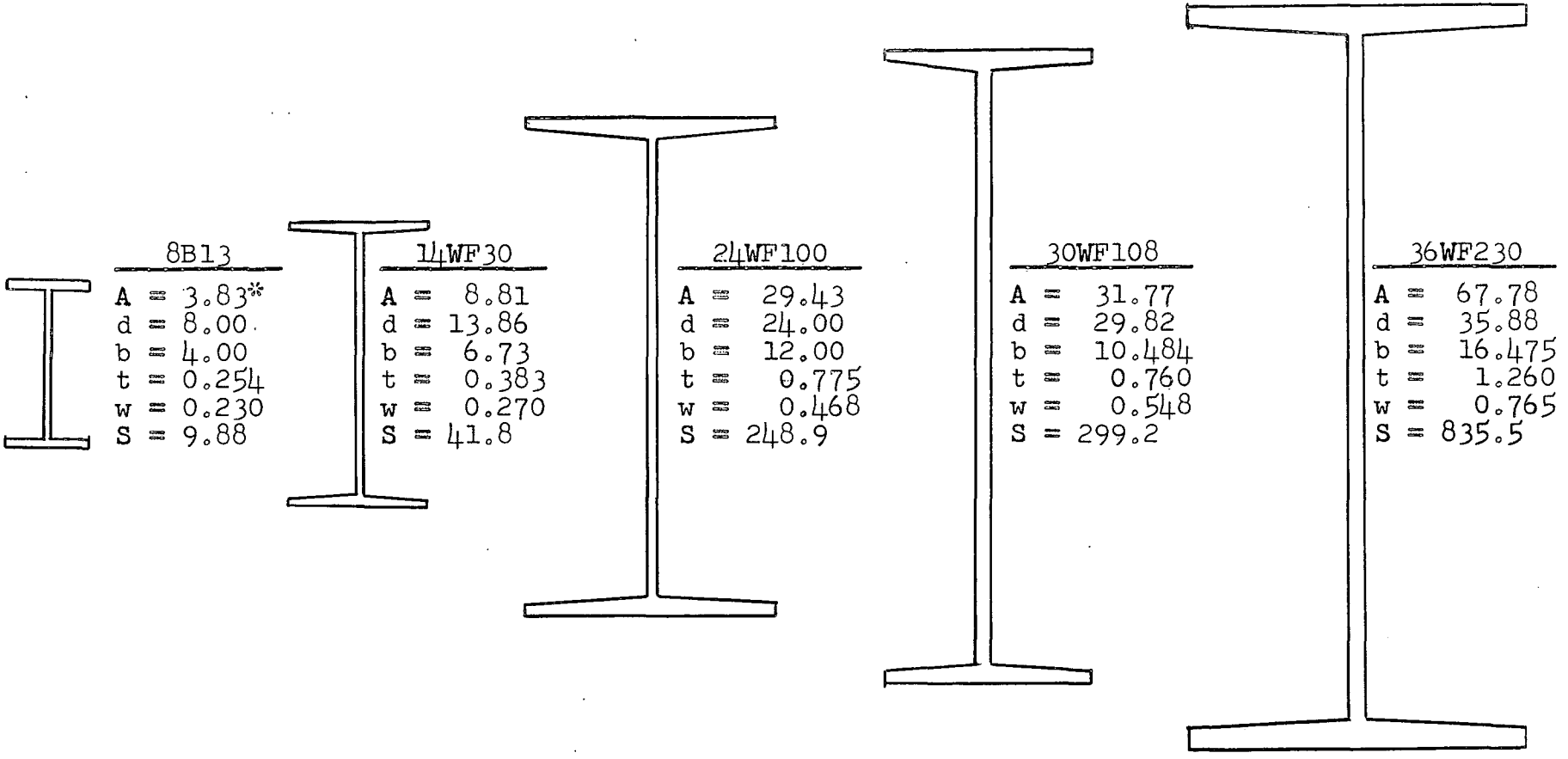

Figure 2
SCALE DRAWING OF CROSS SECTIONS

*All Quantities Are HANDBOOK Values

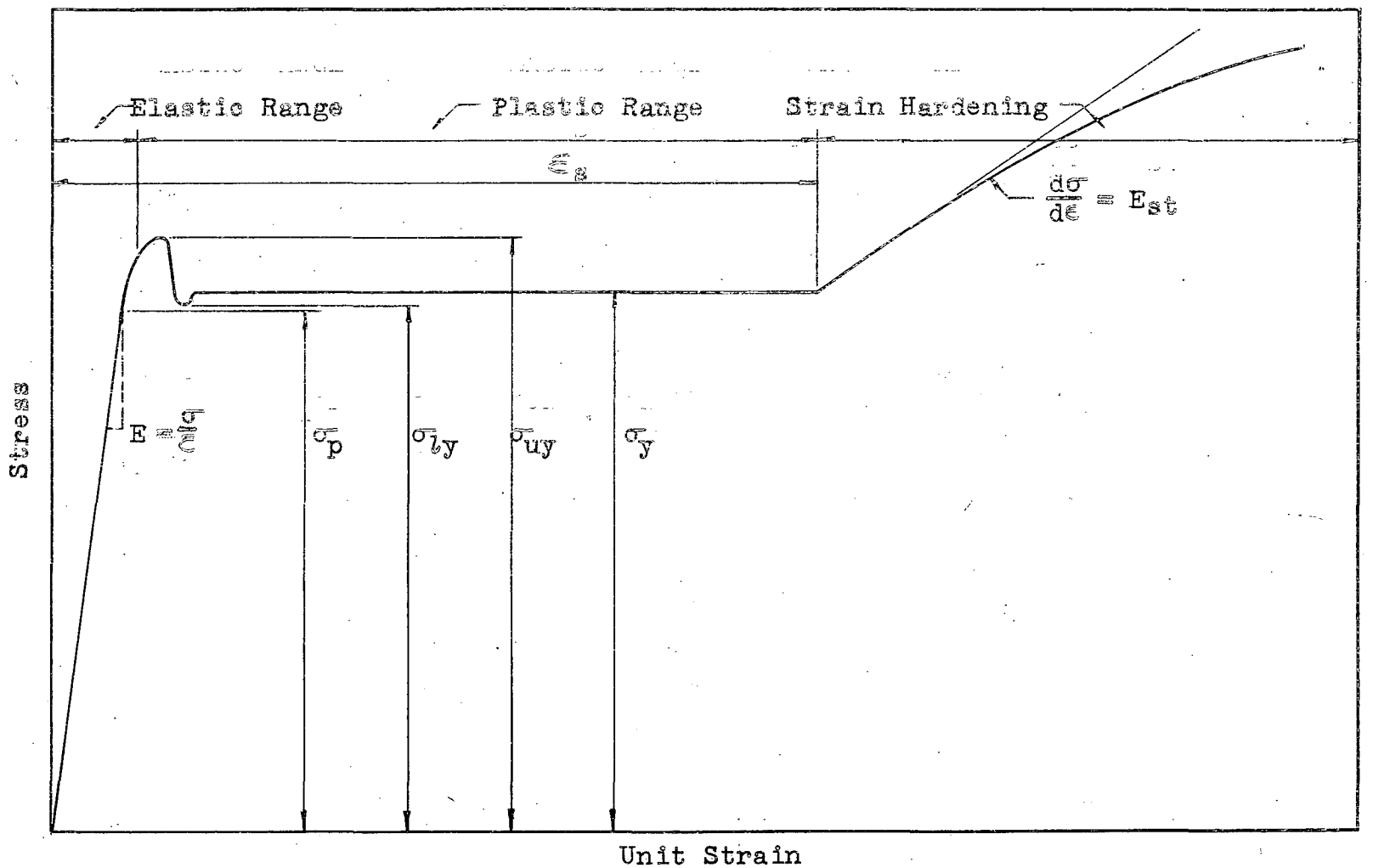

Fig. 3 - DEFINITION OF TERMS

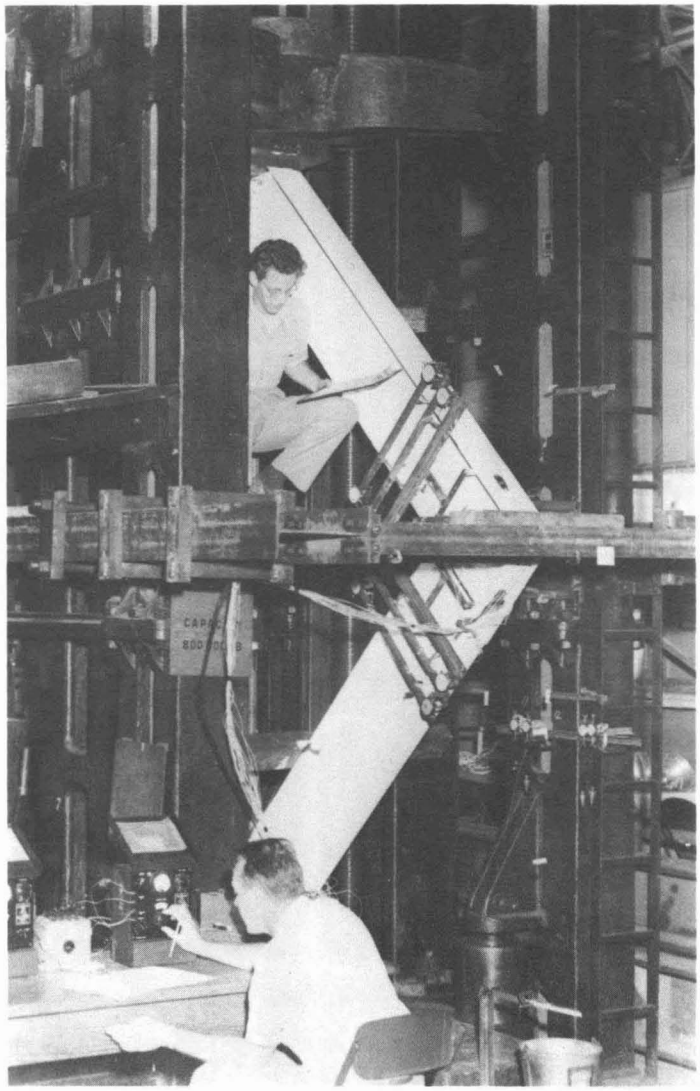

FIG 4 TEST SETUP OF THE 14WF30 CONNECTION IN THE 800,000 TESTING MACHINE SHOWING LATERAL SUPPORT SYSTEM, ROTATION INDICATORS, AND MIRROR GAGE

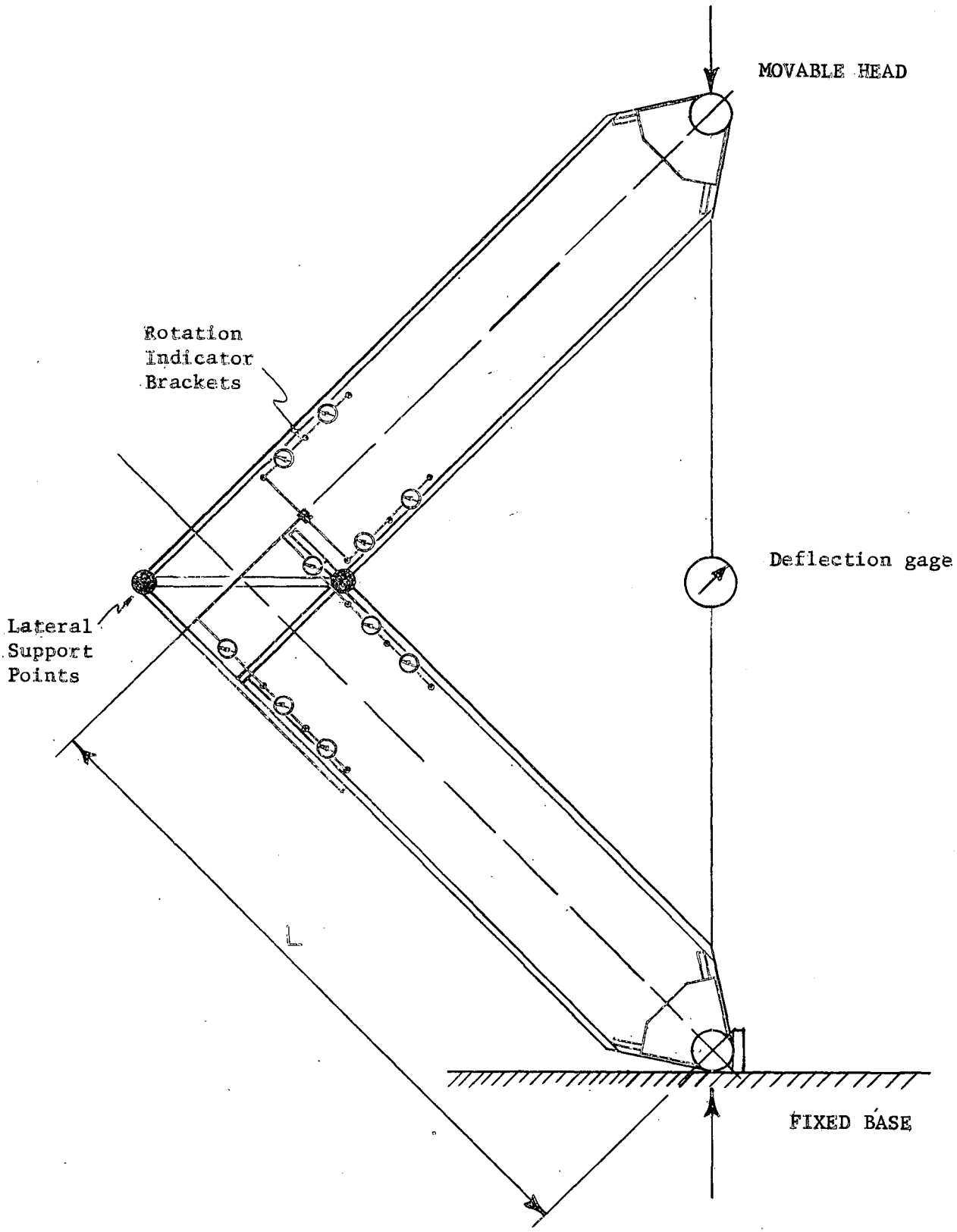

SCHEMATIC DIAGRAM OF TEST SET-UP

Figure 5

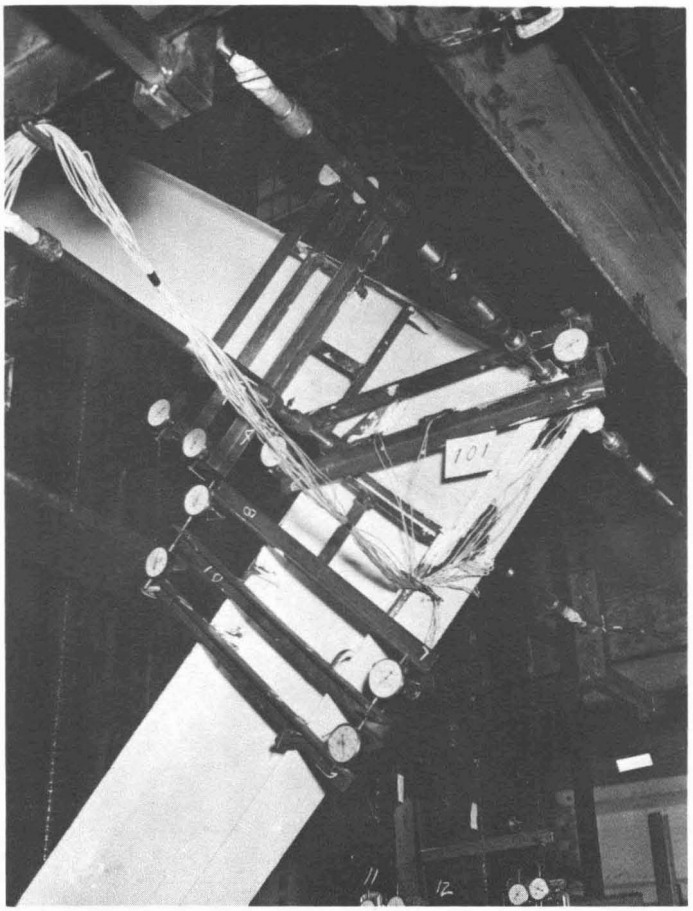

FIG 6 14WF30 CONNECTION SHOWING ROTATION INDICATORS AND BRACKETS AS WELL AS THE LATERAL SUPPORT TIE RODS FITTED WITH FLEX BARS AT EACH END

The following figures may be found in the text on the pages indicated below

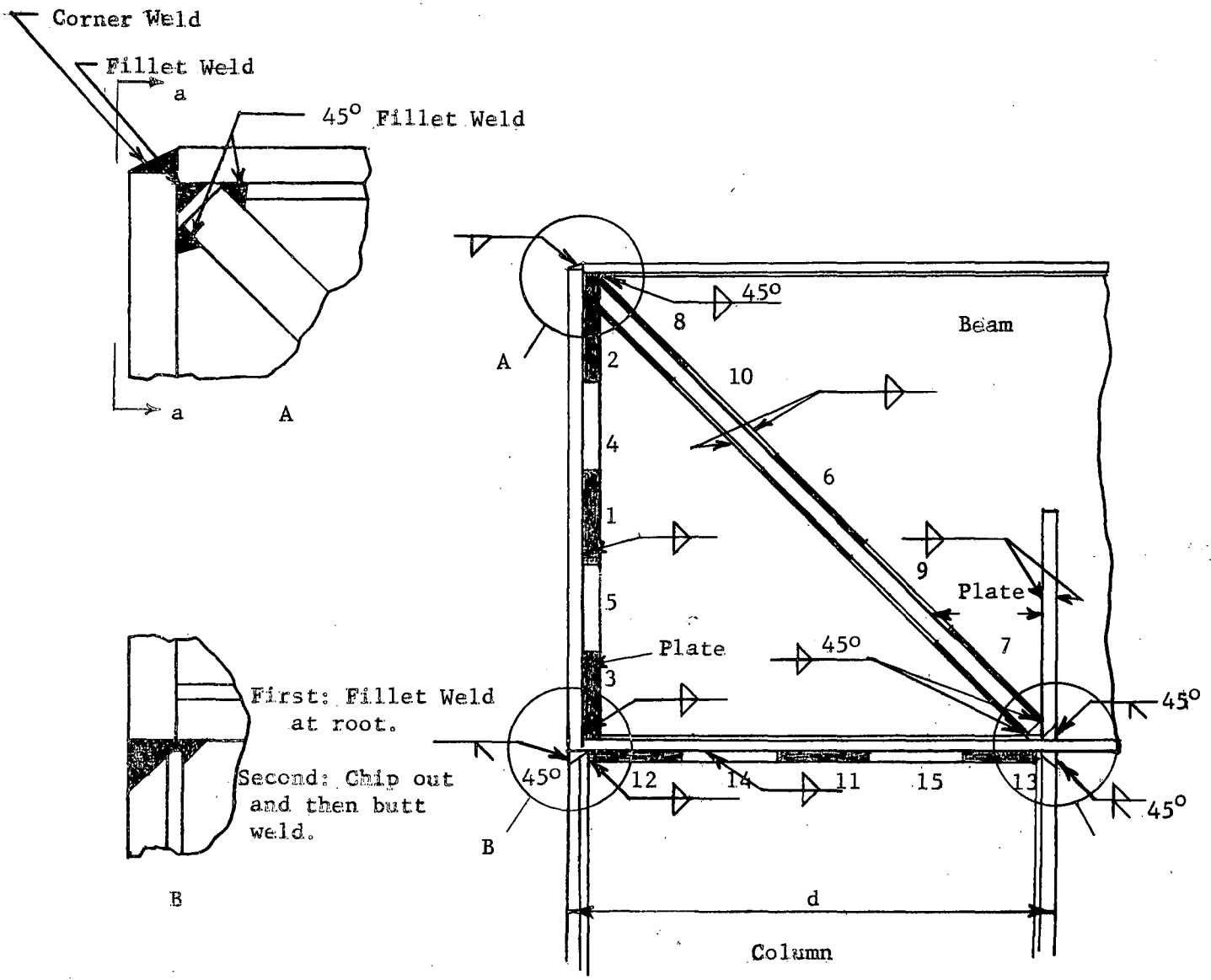

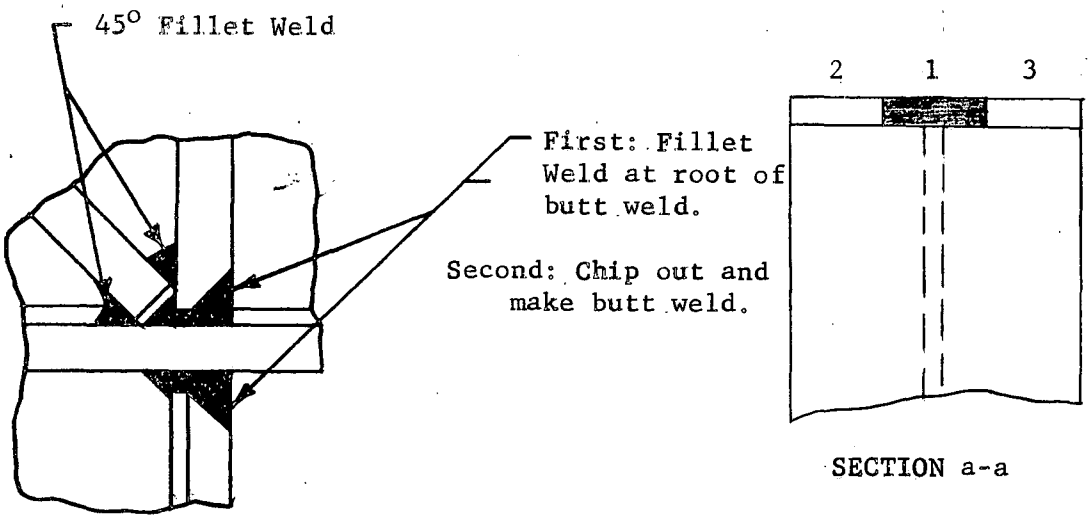

C

WELDING DETAILS
Figure 10

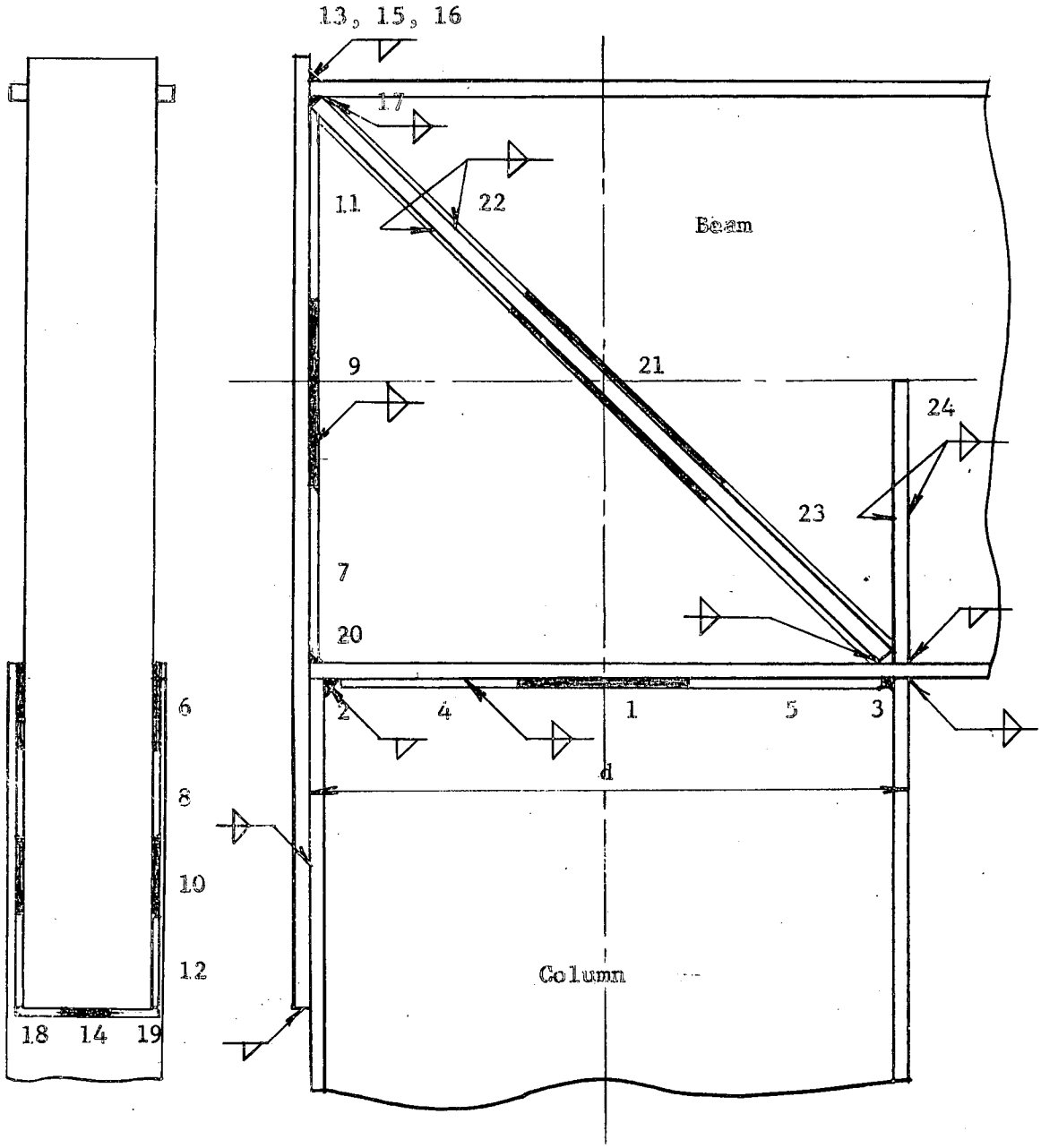

WELDING DETAILS

Figure 11

COMPARISON OF MOMENT-DELFECTION CURVES

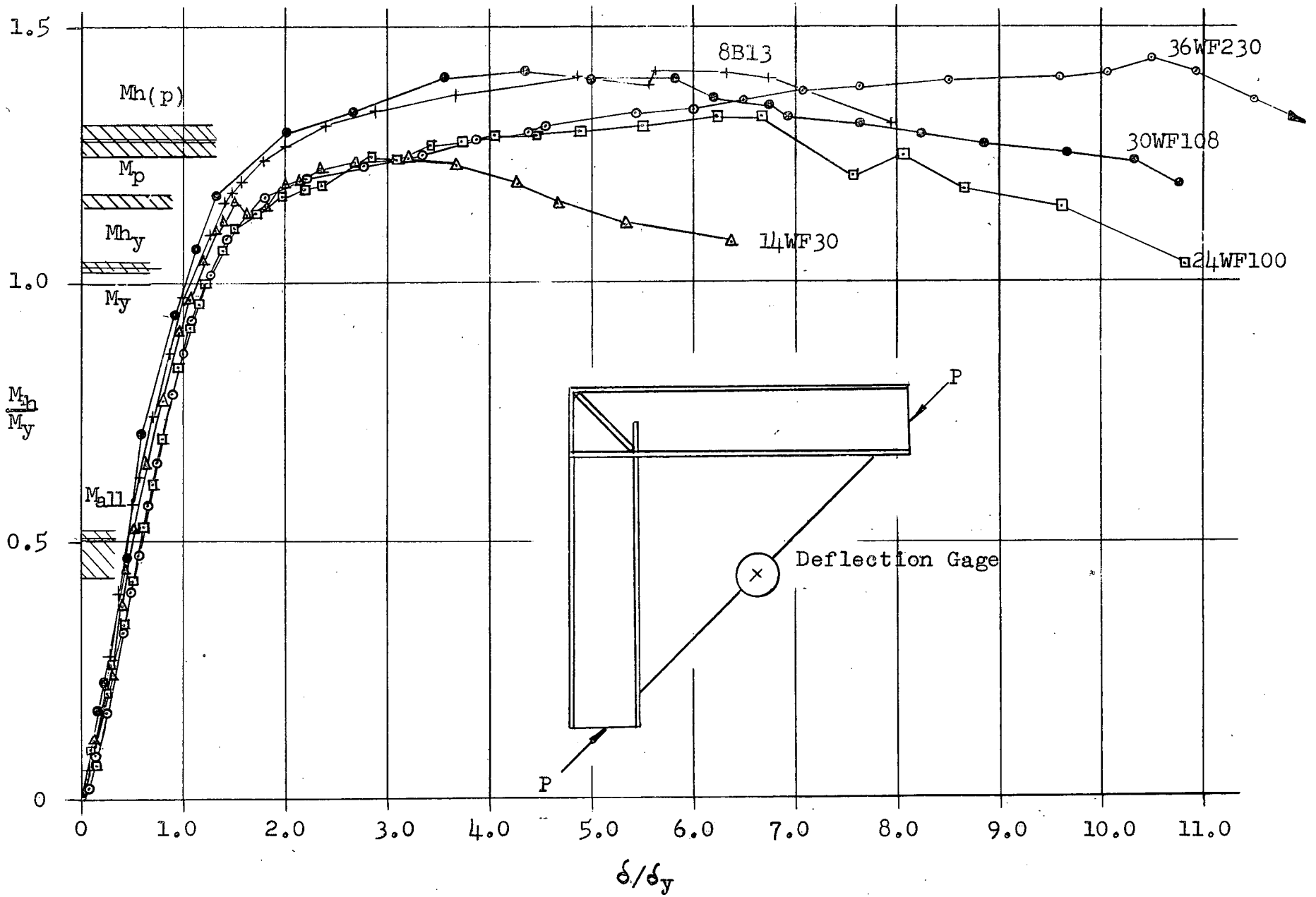

Figure 13

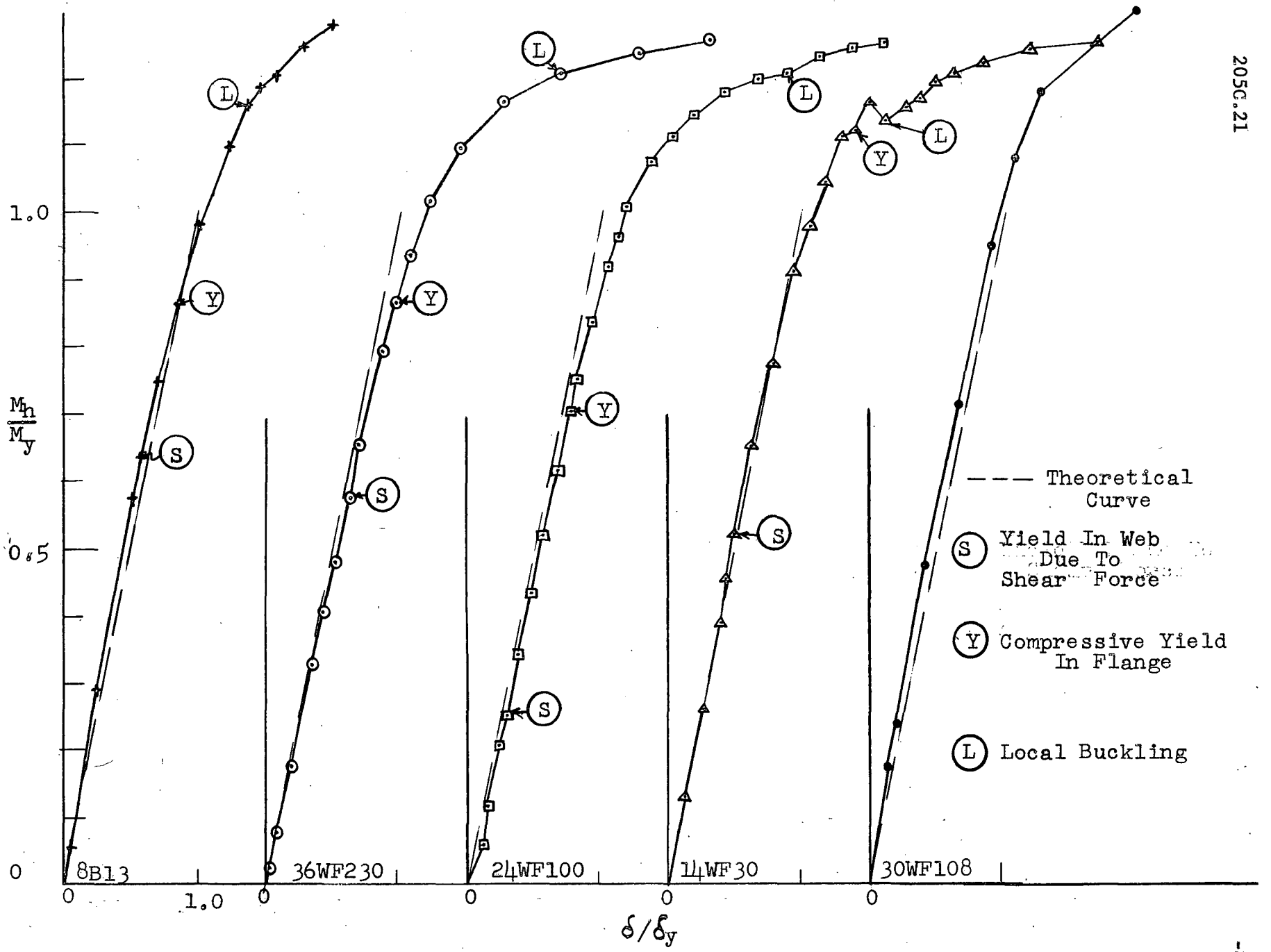
1.0
0.5
0
M_h/M_y
8B13
36WF230
24WF100
14WF30
30WF108
0
1.0
δ/δ_y
L
Y
S
Theoretical Curve
Yield In Web Due To Shear Force
Compressive Yield In Flange
Local Buckling

Figure 14

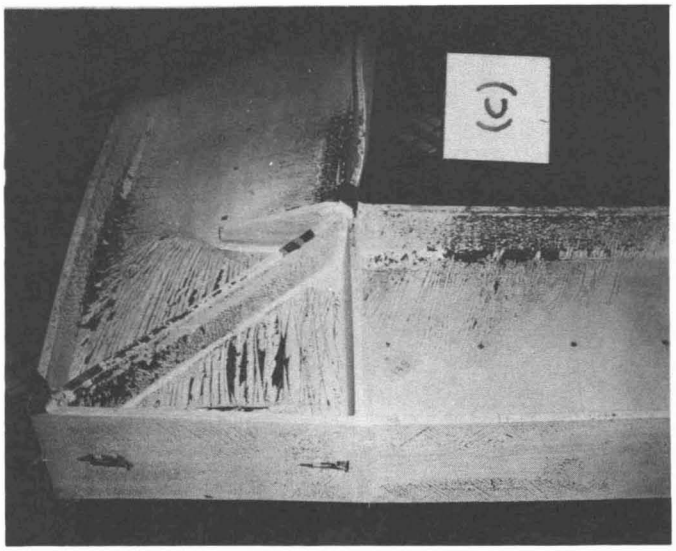

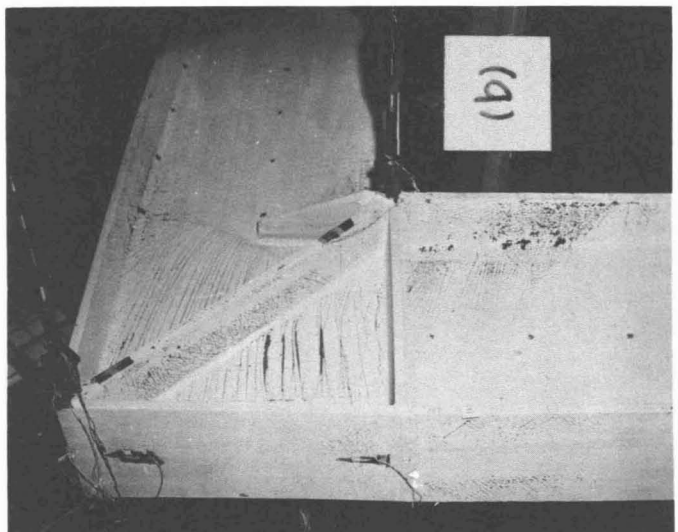

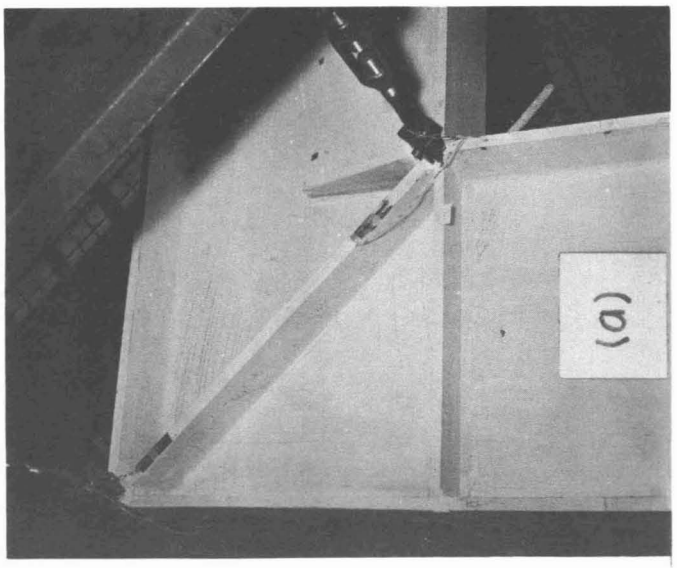

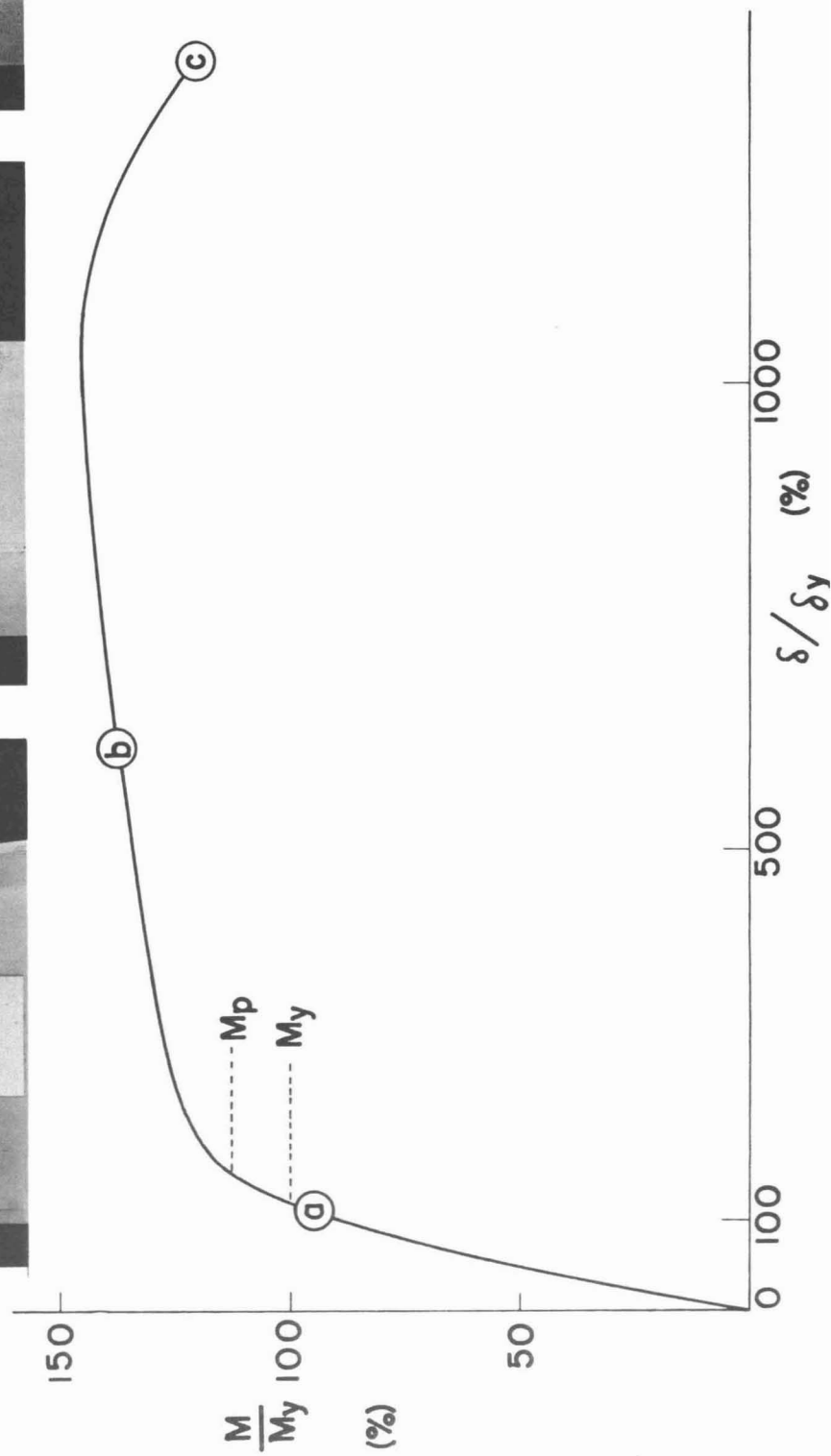

FIG 15

COMPARISON OF MOMENT-ROTATION CURVES

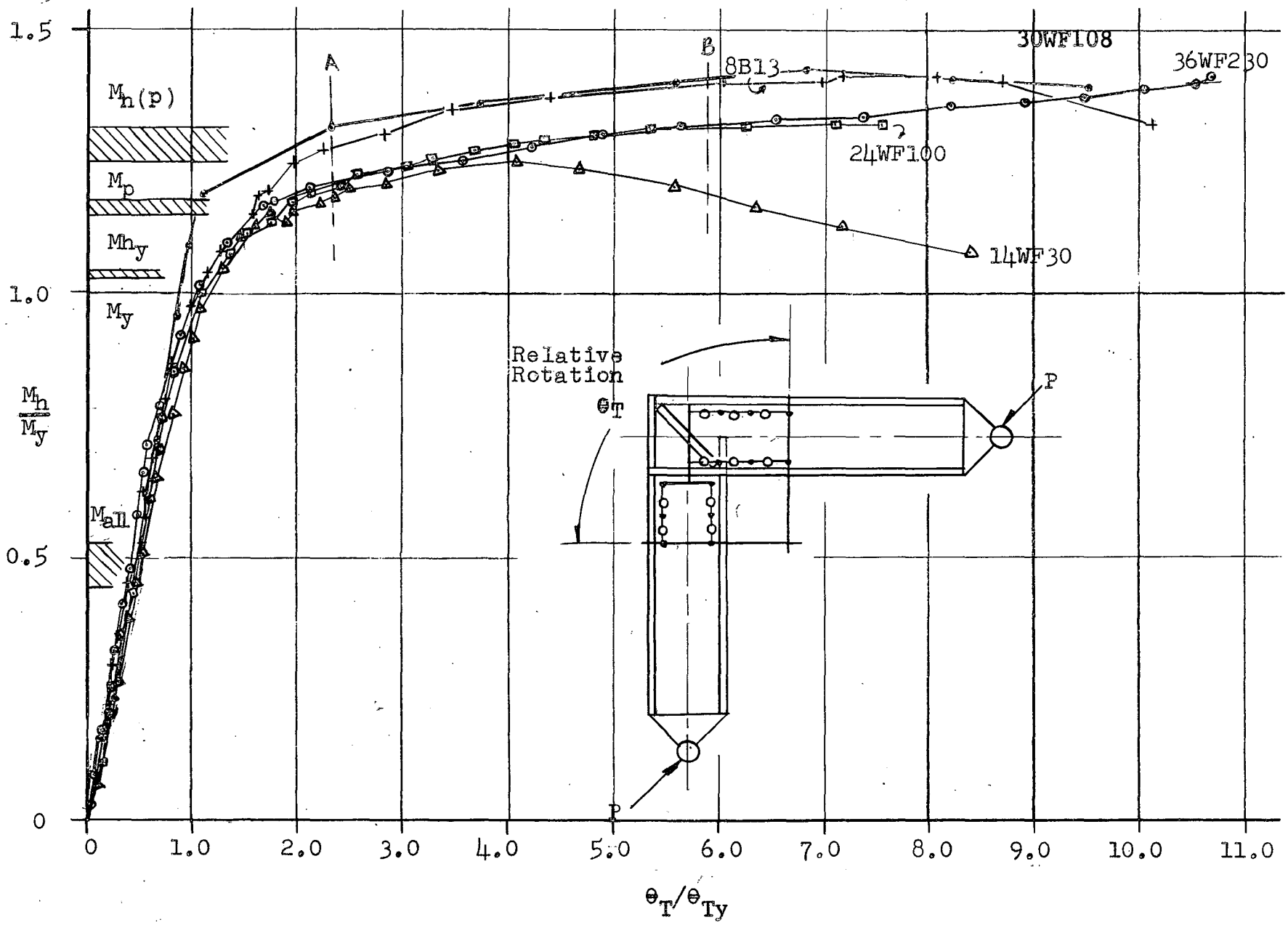

Figure 16

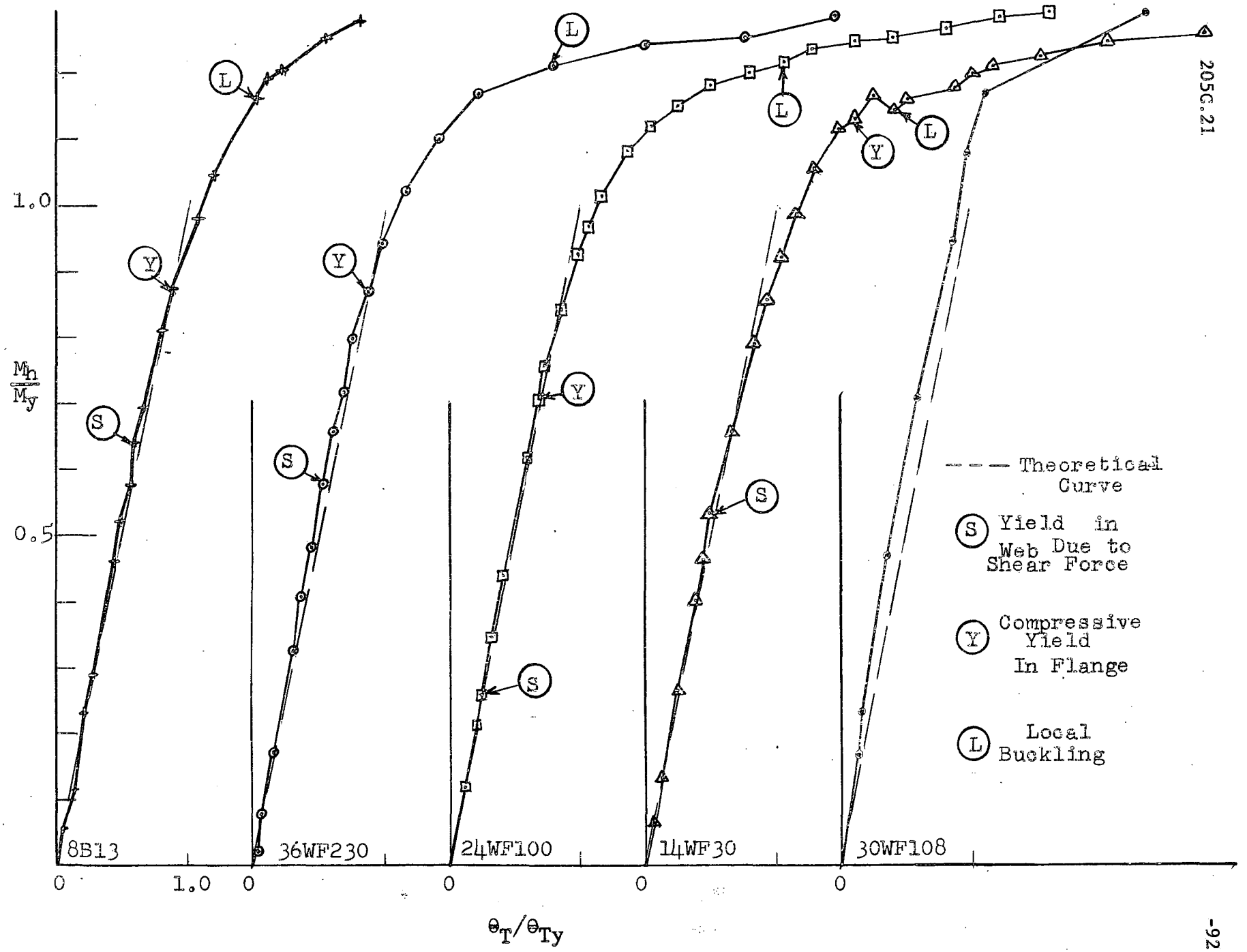
1.0
0.5
M_h/M_y
8B13
36WF230
24WF100
14WF30
30WF108
0
1.0
0
0
0
0
θ_T/θ_{Ty}
S
Y
L
Theoretical Curve
S Yield in Web Due to Shear Force
Y Compressive Yield In Flange
L Local Buckling

Figure 17

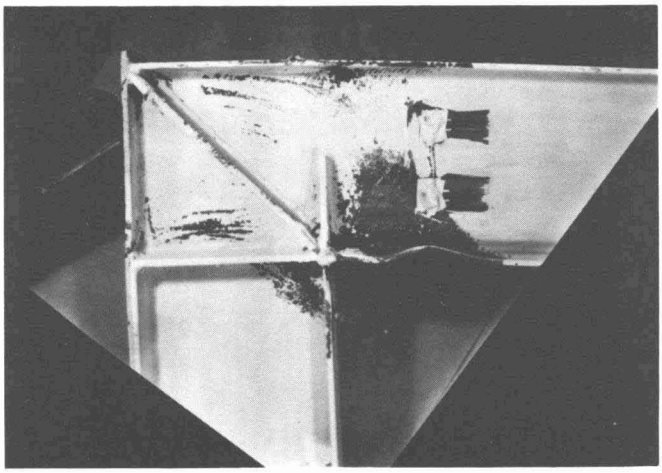

FIG 18 MODE OF FAILURE OF 8B13 CONNECTION SHOWING LOCAL BUCKLING AT END OF TEST. YIELD DUE TO SHEAR CAN BE NOTED IN THE WEB

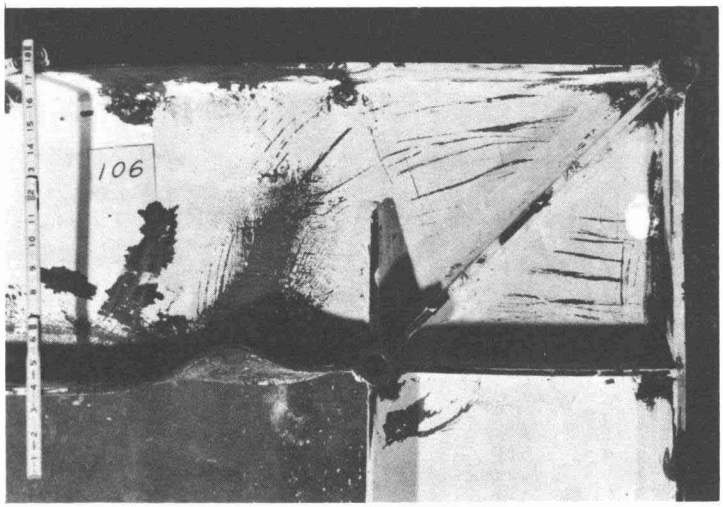

FIG 19 MODE OF FAILURE OF 14WF30 CONNECTION. LOCAL BUCKLING OCCURRED SHORTLY AFTER GENERAL YIELDING, AND WAS CAUSE OF FAILURE

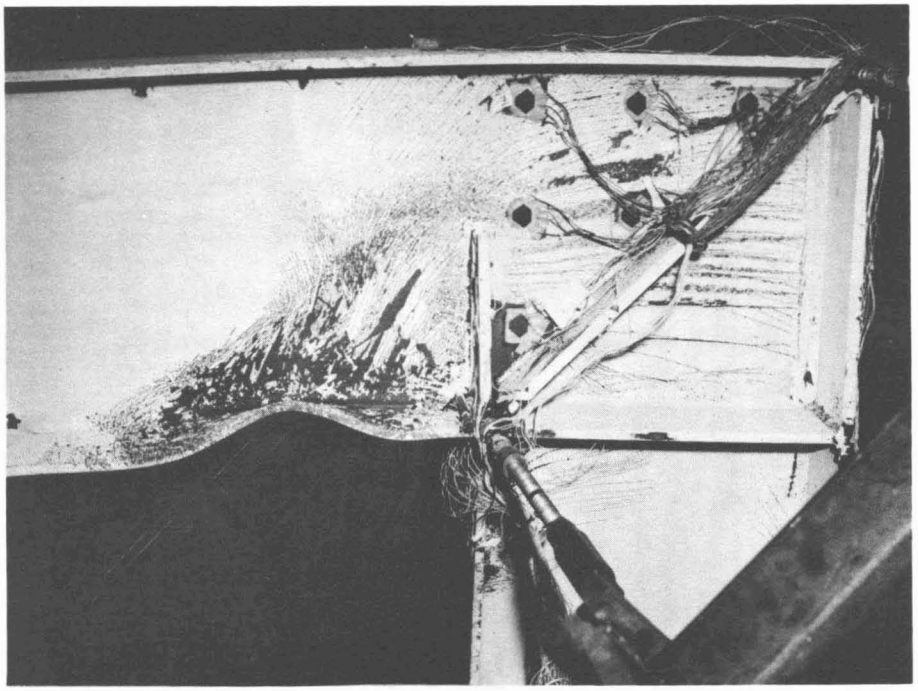

FIG 20 LOCAL BUCKLING OCCURRED AFTER CONSIDERABLE YIELDING IN THE 24 WF100 CONNECTION

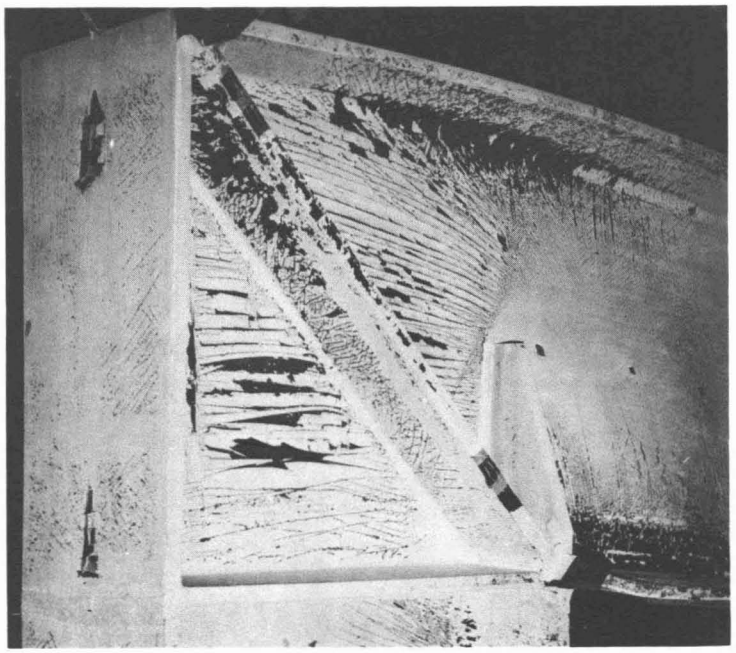

FIG 21 LOCAL BUCKLING AND YIELDING OF THE 36WF 230 CONNECTION AT THE END OF THE TEST

FLANGE BUCKLING CURVES

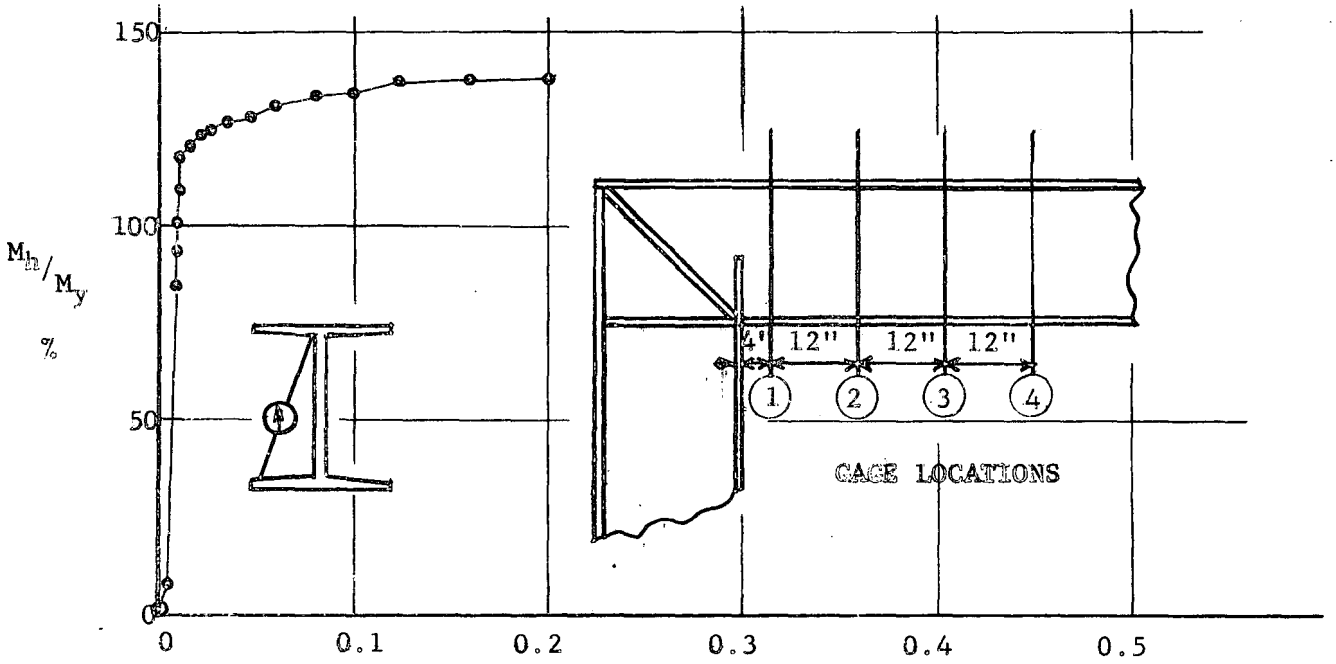

Beam-Flange Deformation (inches) AT GAGE 2

GAGE NO.

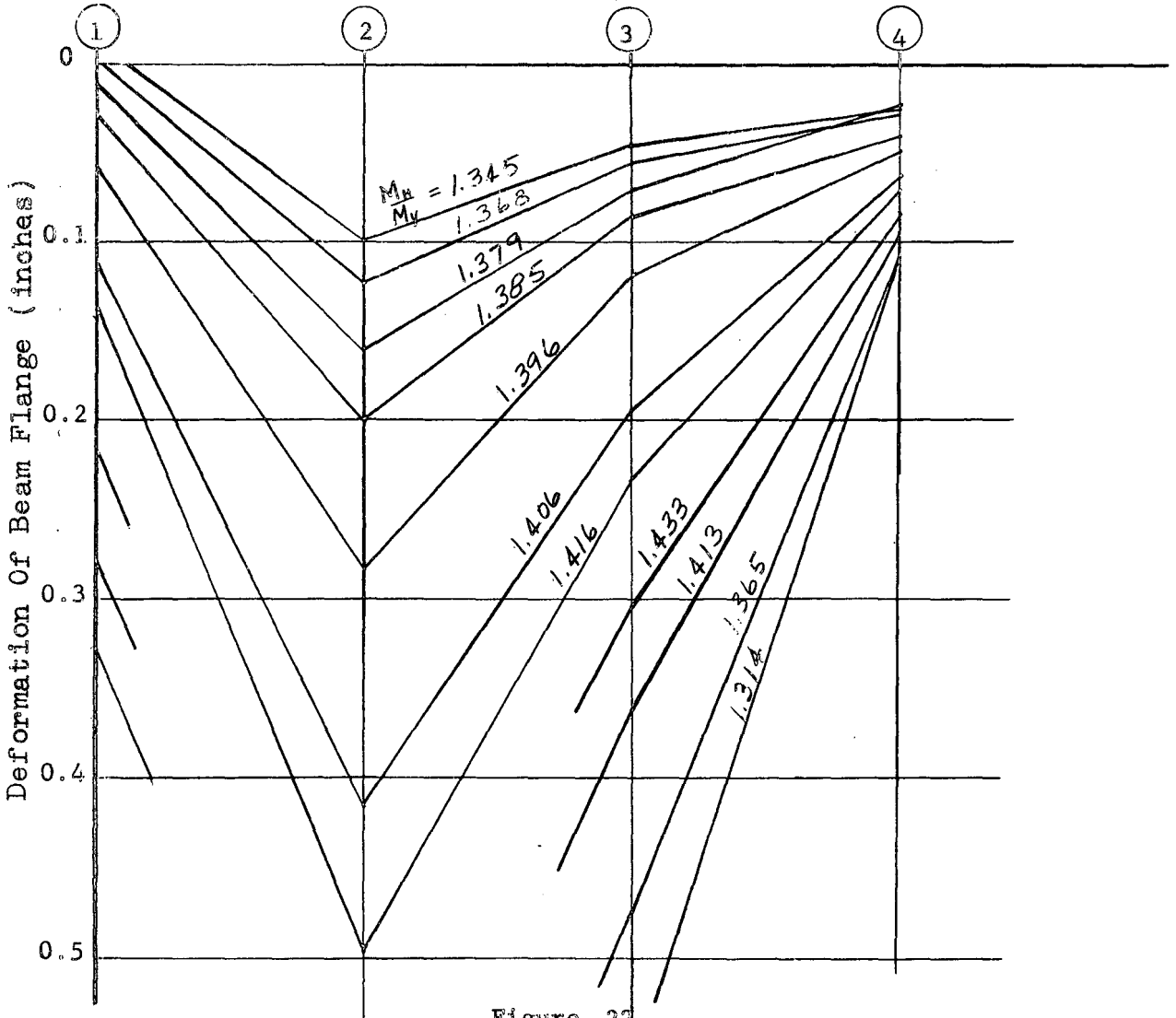

Figure 22

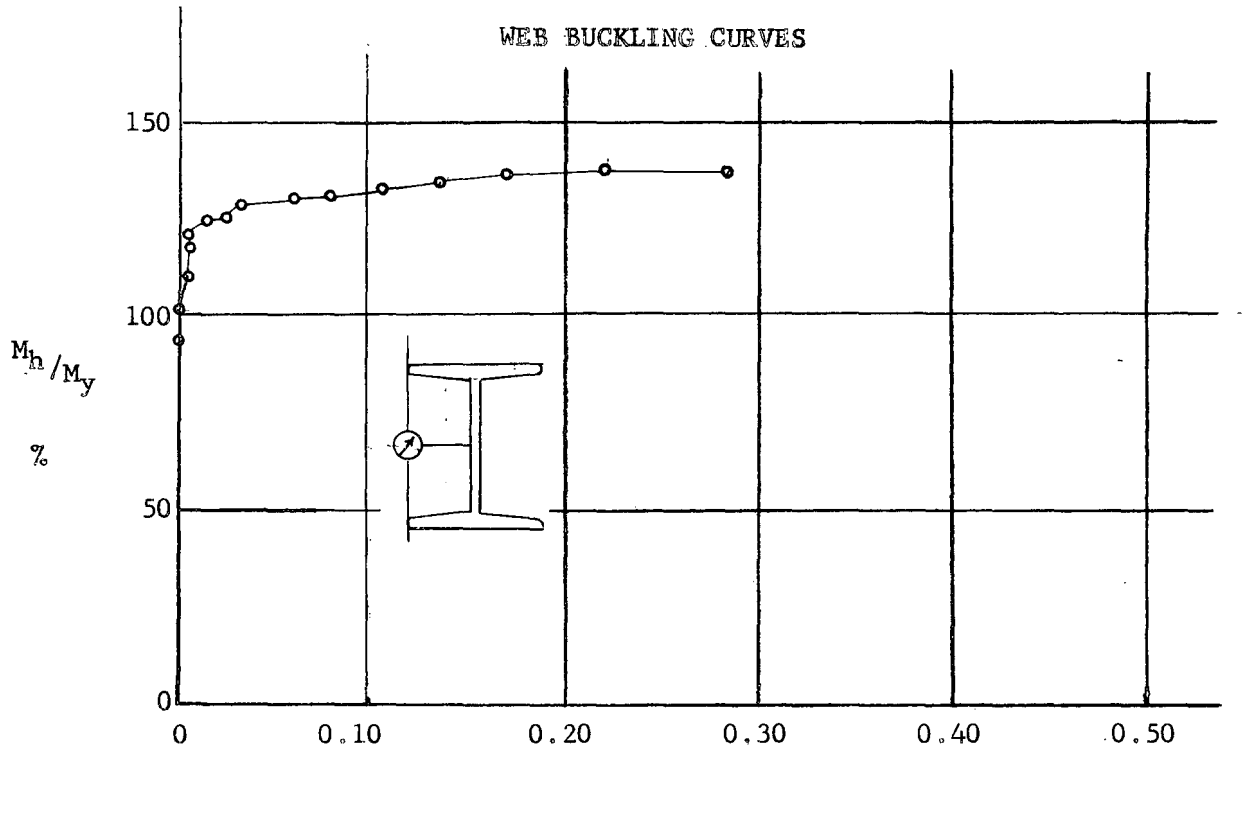
WEB BUCKLING CURVES
150
100
50
0
M_h/M_y
%
0
0.10
0.20
0.30
0.40
0.50
Web deformation (inches) @ GAGE 1

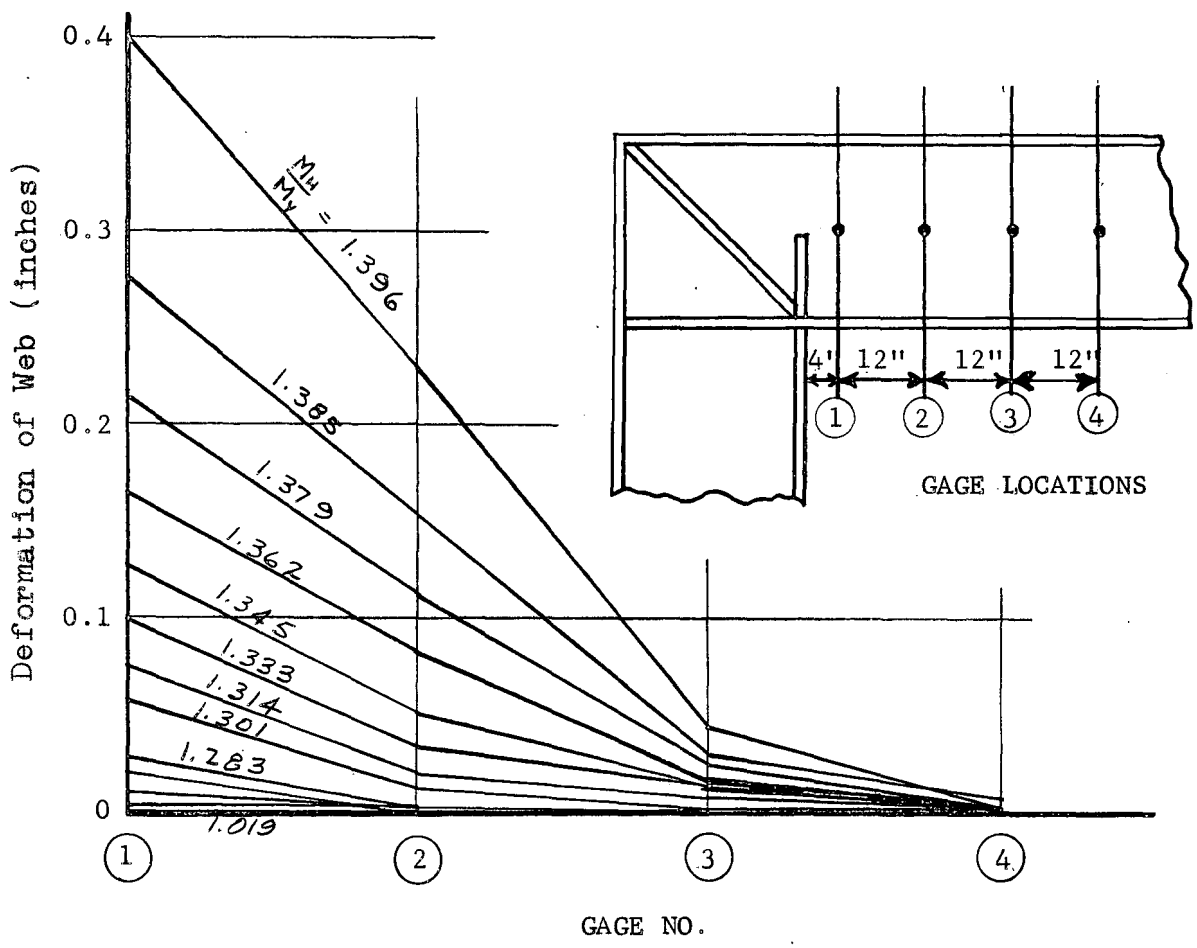
0.4
0.3
0.2
0.1
0
Deformation of Web (inches)
$\frac{M_H}{M_y}$ = 1.396
1.385
1.379
1.362
1.345
1.333
1.314
1.301
1.283
1.019
1
2
3
4
GAGE NO.
4'
12"
12"
12"
GAGE LOCATIONS

Figure 23

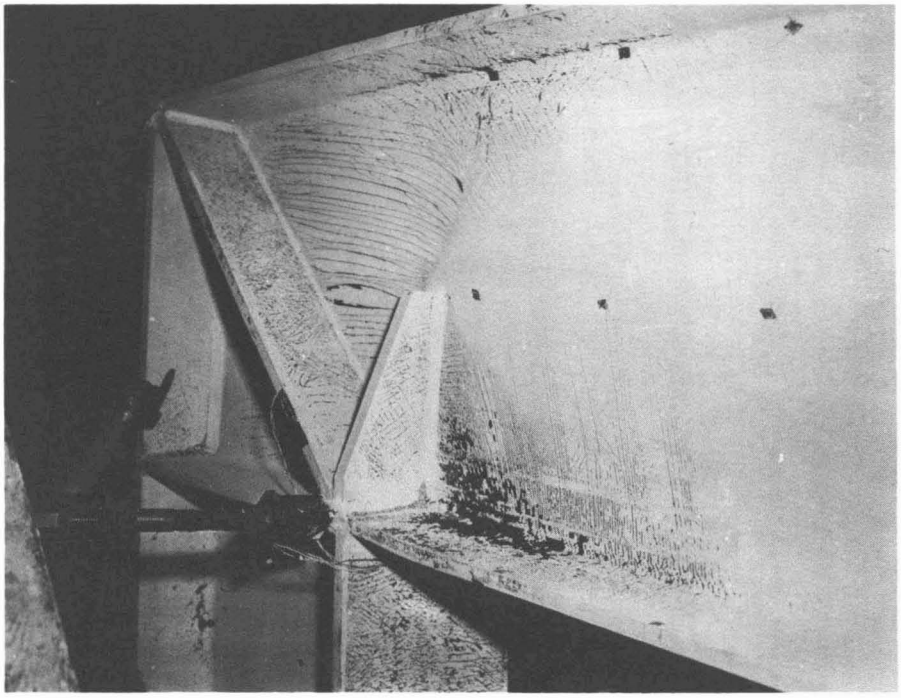

FIG 25 GENERAL YIELDING IN THE WEB, HALF-DEPTH VERTICAL STIFEENER, AND DIAGONAL STIFFENER OF THE 36WF230 CONNECTION. NOTE THE PINS AND CLEVICES AT END OF TIE RODS

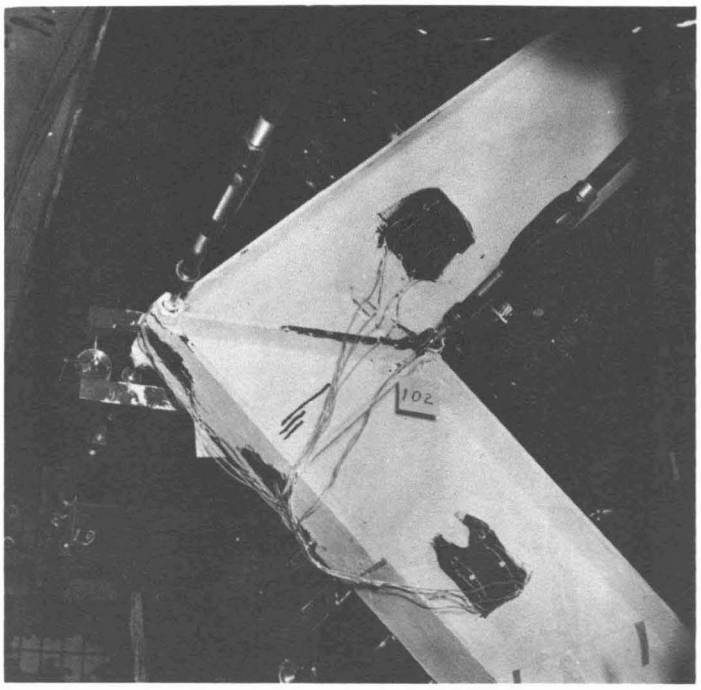

FIG 26 SHEAR YIELD LINES AT 85% OF PREDICTED YIELD LOAD ON 14WF30 CONNECTION. (THE PATTERN HAS BEEN ACCENTUATED BY TRACING THE ORIGINAL LINES IN INK)

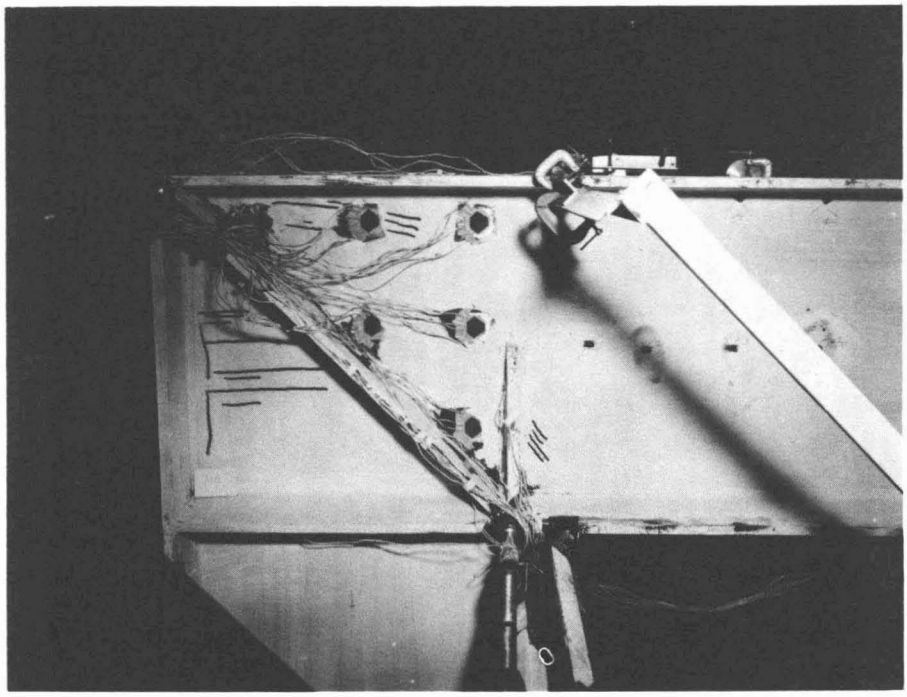

FIG 27 CLOSEUP OF 24WF100 CONNECTION SHOWING SHEAR YIELD LINES AT ABOUT 73% OF PREDICTED YIELD LOAD (THE PATTERN HAS BEEN ACCENTUATED BY TRACING THE ORIGINAL LINES IN INK)

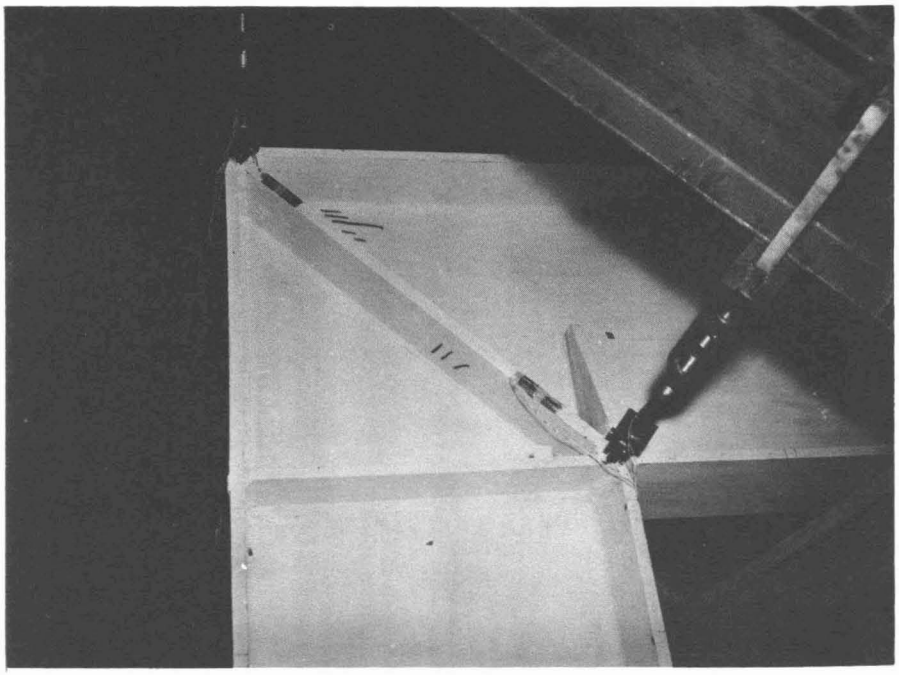

FIG 28 36 WF 230 CONNECTION AT ABOUT 50% OF PREDICTED YIELD LOAD. NOTE THE SHEAR YIELD LINES IN WEB NEAR OUTSIDE CORNER AND ON DIAGONAL STIFFENER